

國立交通大學

電子工程學系 電子研究所碩士班

碩士論文

高介電常數材料氧化鋁在矽基板上之界面特性研究



**The Interface Investigation of High-K Material  $\text{Al}_2\text{O}_3$   
on Si Substrate**

研究生：謝文斌

指導教授：羅正忠 博士

中華民國九十三年六月

高介電常數材料氧化鋁在矽基板上  
之介面特性研究

**The Interface Investigation of High-K Material Al<sub>2</sub>O<sub>3</sub>  
on Si Substrate**

研究生：謝文斌

Student : Wen-Bin Shie

指導教授：羅正忠 博士

Advisor : Dr. Jen-Chung Lou

國立交通大學

電子工程學系

電子研究所碩士班



碩士論文

A Thesis

Submitted to Institute of Electronics  
College of Electrical Engineering and Computer Science  
National Chiao Tung University  
in Partial Fulfillment of the Requirements  
for the Degree of  
Master of Science  
in  
Electronic Engineering  
June 2004  
Hsinchu, Taiwan, Republic of China

中華民國 九十三年 六月

# 高介電常數材料氧化鋁在矽基板上之界面特性研究

研究生:謝文斌

指導教授:羅正忠 博士

國立交通大學

電子工程學系

電子研究所碩士班



根據半導體的微縮定律，隨著半導體製造逐漸的微小化，極薄的二氧化矽介電層將伴隨著極大的直接穿遂漏電流，而這個直接穿遂漏電流將對元件的功率消耗有嚴重的影響。在閘極二氧化矽介電層薄到 10 奈米以下的情況之下，為了解決這嚴重的直接穿遂漏電流現象，我們將利用高介電係數材料來替換傳統的二氧化矽。我們利用高介電係數材料在相同的等效二氧化矽厚度之下，能擁有較大的實際物理厚度以抵擋直接穿遂漏電流。

在眾多高介電係數材料之中，氧化鋁是一種非常有潛力的高介電係數材料。它有較高的介電係數（約 8~10），足夠高的載子能障（對

電子約 2.9 電子伏特，對電洞約 4.3 電子伏特)，以及與矽有著良好的熱穩定性。在論文中，我們研究氧化鋁經由  $\text{NH}_3$  表面處理與在氧氣與氮氣環境下進行沈積後退火 (PDA) 在物性，電性，及可靠度分析。沈積後退火 (PDA) 可以有效的降低表面粗糙度。我們發現  $\text{NH}_3$  表面處理與沈積後退火 (PDA) 都能改善試片在電容-電壓電性分析上的平台現象，其中氮氣表面處理更可以降低試片的漏電流。

有先經過  $\text{NH}_3$  表面處理與在氮氣環境下進行沈積後退火 (PDA) 的話，其介電質的可靠度將會變得較佳。在氧化鋁薄膜內的漏電傳導機制是由 Schottky 發射所主導的。綜上所述，氧化鋁介電層的特性在  $\text{NH}_3$  表面處理配合後續沈積後退火處理後得到了有效的改善。這種新穎的  $\text{NH}_3$  表面處理與沈積後退火提供了未來奈米元件應用在金氧半沈積處理上一個極佳的選擇。

# The Interface Investigation of High-K Material Al<sub>2</sub>O<sub>3</sub> on Si Substrate

Student : Wen-Bin Shie

Advisor : Dr. Jen-Chung Lou

Department of Electronics Engineering and Institute of Electronics

National Chiao Tung University, Hsinchu, Taiwan



According to the scaling rules, aggressive scaling has led to silicon dioxide (SiO<sub>2</sub>) gate dielectrics as ultra thin in state-of-the-art CMOS technologies. As a consequence, static leakage power due to direct tunneling through the gate oxide has been increasing at an exponential rate. As technology roadmaps call for sub-10Å gate oxides within the next five years, a variety of alternative high-*k* materials are being investigated as possible replacements for SiO<sub>2</sub>. The higher dielectric constants in these materials allow the use of physically thicker films, potentially reducing the tunneling current while maintaining the gate capacitance needed for scaled device operation.

Aluminum oxide ( $\text{Al}_2\text{O}_3$ ) is one of the potential high- $k$  materials. It has the higher dielectric constant (8~10), higher barrier height ( 2.9eV for electrons , and 4.3eV for holes ), and excellent thermal stability. In the thesis, physical, electrical and reliability characteristics of  $\text{Al}_2\text{O}_3$  film with  $\text{NH}_3$  surface treatment and Post Deposition Annealing (PDA) in the  $\text{O}_2$  and  $\text{N}_2$  ambient were studied. The PDA can effectively reduce surface roughness. The PDA and  $\text{NH}_3$  surface treatments both can improve the C-V curves. Moreover, the lower leakage current is observed in  $\text{NH}_3$  surface treatment samples.

The reliabilities can be improved by the  $\text{NH}_3$  surface treatment after PDA in a  $\text{N}_2$  ambient. The conduction mechanism in the  $\text{Al}_2\text{O}_3$  thin film is dominated by the Schottky emission. To sum up, the characteristics of  $\text{Al}_2\text{O}_3$  gate dielectrics with  $\text{NH}_3$  surface treatment and subsequent PDA treatment described above are effectively improved. This novel  $\text{NH}_3$  and PDA treatment provides an alternative for post metal-oxide deposition treatment in nanoscale device application.

## 誌 謝

在長達十多年的學生生涯中，終於要在交通大學碩士班暫時劃下句點了，首先要感謝我的爸媽給我無微不至的照顧與全心全力讓我無後顧之憂的支持。然後，在兩年的碩士生涯中，我要感謝我的指導教授羅正忠博士，由於有老師在研究上給予我細心的指導及教誨，讓我在學術及研究上都有莫大的收穫，讓我受益良多並更加成長，在這裡對老師致上內心最誠摯的敬意與謝意。此外，我要感謝陳永裕與陳世璋兩位學長，謝謝你們提供我諸多的專業指導及協助，並不厭其煩的幫助我解決實驗上的問題，讓我能順利地完成研究，並在我實驗遇到困難的時候，給予我相當寶貴的意見與指教，沒有你們的幫助這篇論文是沒辦法順利完成的，謝謝你們。同時，也要感謝曾經一起打拼的同學們：元均、榮祥、國欽、俊彥，謝謝你們在課業及生活上的陪伴與砥礪，也感謝你們所提供的每一項幫助與鼓勵。也要感謝彥廷、昶維、宗翰、祐慈、雁雅...等學弟妹的協助。最後還要感謝我的女朋友：欣穎及一群從大學以來就一直陪伴我的好朋友：志豪、宗育、國誠，有你們一起度過的大學及研究生生活，實在是我生命中最美好的一段回憶。另外，我要感謝國家奈米元件實驗室(NDL)與交大奈米中心提供良好的設備與其中每一位勞苦功高的工作人員所給予的幫助，讓我能順利的完成實驗。總之，真的要謝謝我所遇見的每一個人，沒有你們就不會有現在的我，在此獻上內心最深的謝意，謝謝你們～

# Contents

<b>Abstract (Chinese)</b> .....	i
<b>Abstract (English)</b> .....	iii
<b>Acknowledgements</b> .....	v
<b>Contents</b> .....	vi
<b>Table Captions</b> .....	viii
<b>Figure Captions</b> .....	ix

## Chapter 1 Introduction

1.1 General Background.....	1
1.2 Motivation.....	3
1.3 Characterization of Al <sub>2</sub> O <sub>3</sub> .....	4



## Chapter 2 Basic Characteristics of Al<sub>2</sub>O<sub>3</sub> Gate Dielectrics Using Rapid Thermal Annealing Technology

2.1 Introduction.....	9
2.2 Experiment.....	10
2.3 Results and discussion	
2.3-1 Capacitance-Voltage characteristic.....	10
2.3-2 Current density-Electric field characteristic.....	11
2.3-3 Time dependent dielectric breakdown.....	12
2.3-4 Surface morphology.....	13



2.4	Summary.....	14
<b>Chapter 3</b>	<b>Characteristics of Al<sub>2</sub>O<sub>3</sub> Gate Dielectrics Using NH<sub>3</sub> Surface Nitridation Technology</b>	
3.1	Introduction.....	22
3.2	Experiment.....	23
3.3	Results and discussion	
3.3-1	Capacitance-Voltage characteristic.....	24
3.3-2	Current density-Electric field characteristic.....	25
3.3-3	Time dependent dielectric breakdown.....	26
3.3-4	Conduction mechanism.....	28
3.4	Summary.....	30
<b>Chapter 4</b>	<b>Conclusions and Suggestions for Future Work</b>	
4.1	Conclusions.....	40
4.2	Suggestions for Future Work .....	41
References	.....	43

# Table Captions

## Chapter 1

Table 1.1 Basic properties of current high-k candidates

Table 1-2 Material properties of  $\text{Al}_2\text{O}_3$ ,  $\text{ZrO}_2$ ,  $\text{HfO}_2$ [3]

## Chapter 2

## Chapter 3

Table.3-1(a) The experimental  $\beta$  and Schottky barrier high of  $\text{Al}_2\text{O}_3$  samples with  $\text{NH}_3$  and w/o  $\text{NH}_3$  treatment after PDA  $900^\circ\text{C}$  in an  $\text{O}_2$  ambient

Table.3-1(b) The experimental  $\beta$  and Schottky barrier high of  $\text{Al}_2\text{O}_3$  samples with  $\text{NH}_3$  and w/o  $\text{NH}_3$  treatment after PDA  $900^\circ\text{C}$  in a  $\text{N}_2$  ambient

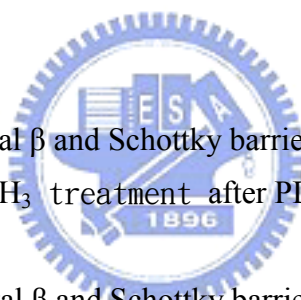


# Figure Captions

## Chapter 1

Fig 1-1 the expected equivalent oxide thickness ( EOT ) trends from the published  
2003- ITRS roadmap

Fig 1-2 Band alignment of topical high-k dielectrics

## Chapter 2

Fig.2-1 Process flows of experimental samples

Fig.2-2 The C-V curves of Al<sub>2</sub>O<sub>3</sub> samples annealing in an O<sub>2</sub> ambient

Fig.2-3 The C-V curves of Al<sub>2</sub>O<sub>3</sub> samples annealing in a N<sub>2</sub> ambient

Fig.2-4 The CET of Al<sub>2</sub>O<sub>3</sub> samples after various post annealing temperature  
750°C, 850°C, 950°C

Fig.2-5 The J-E curves of Al<sub>2</sub>O<sub>3</sub> samples with various PDA temperature in an O<sub>2</sub>  
ambient.

Fig.2-6 The J-E curves of Al<sub>2</sub>O<sub>3</sub> samples with various PDA temperature in a N<sub>2</sub>  
ambient.

Fig.2- 7 The J at V<sub>g</sub>= -1 V of Al<sub>2</sub>O<sub>3</sub> samples with various PDA temperature

Fig.2- 8 The Weibull plot versus the charge to breakdown Q (C/cm<sup>2</sup>) of Al<sub>2</sub>O<sub>3</sub>  
samples with various PDA temperature in an O<sub>2</sub> ambient.

Fig.2- 9 The Weibull plot shows the charge to breakdown Q (C/cm<sup>2</sup>) of Al<sub>2</sub>O<sub>3</sub>

samples with various PDA temperature in a N<sub>2</sub> ambient.

Fig.2-10 AFM images of Al<sub>2</sub>O<sub>3</sub> with various PDA: (a) As deposition, (b) O<sub>2</sub>-900°C, and (c)N<sub>2</sub>-900°C

Fig.2-11 Leakage current density, R<sub>ms</sub> values versus PDA temperature in an O<sub>2</sub> ambient

Fig.2-12 Leakage current density, CET and R<sub>ms</sub> values versus PDA temperature in a N<sub>2</sub> ambient

### Chapter 3

Fig.3-1 Process flows of experimental samples

Fig.3-2 C-V curve of Al<sub>2</sub>O<sub>3</sub> sample with surface treatment compare to Al<sub>2</sub>O<sub>3</sub> sample without surface treatment after PDA 900°C in an O<sub>2</sub> ambient .

Fig.3-3 C-V curve of Al<sub>2</sub>O<sub>3</sub> sample with surface treatment compare to Al<sub>2</sub>O<sub>3</sub> sample without surface treatment after PDA 900°C in a N<sub>2</sub> ambient

Fig3-4 CET versus Optical thickness of Al<sub>2</sub>O<sub>3</sub> sample with surface treatment compare to Al<sub>2</sub>O<sub>3</sub> sample without surface treatment after PDA 900°C in an O<sub>2</sub> ambient

Fig3-5 CET versus Optical thickness of Al<sub>2</sub>O<sub>3</sub> sample with surface treatment compare to Al<sub>2</sub>O<sub>3</sub> sample without surface treatment after PDA 900°C in a N<sub>2</sub> ambient

Fig3-6-(a) The gate leakage current density (J) versus electric field (E) curves for NH<sub>3</sub> nitrided and w/o NH<sub>3</sub> nitrided after PDA 900°C in an O<sub>2</sub> ambient

Fig3-6-(b) The gate leakage current density (J) versus electric field (E) curves for

NH<sub>3</sub> nitrated and w/o NH<sub>3</sub> nitrated after PDA 900°C in a N<sub>2</sub> ambient

Fig3-7 Current density at  $V_g = -1V$  versus CET curves for NH<sub>3</sub> treatment and without NH<sub>3</sub> treatment.

Fig3-8-(a) The weibull plot shows charge to breakdown for Al<sub>2</sub>O<sub>3</sub> samples with NH<sub>3</sub> and w/o NH<sub>3</sub> treatment at PDA after PDA 900°C in an O<sub>2</sub> ambient

Fig3-8-(b) The weibull plot shows charge to breakdown for Al<sub>2</sub>O<sub>3</sub> samples with NH<sub>3</sub> and w/o NH<sub>3</sub> treatment at PDA after PDA 900°C in a N<sub>2</sub> ambient

Fig3-9 Measured Weibull slopes are plotted versus the physical layer thickness, and a clear gap between the slopes for SiO<sub>2</sub> and the high-k layers can be observed.[20]

Fig3-10(a) The conduction mechanism fitting of Al<sub>2</sub>O<sub>3</sub> samples with NH<sub>3</sub> and w/o NH<sub>3</sub> treatment after PDA 900°C in an O<sub>2</sub> ambient

Fig3-10(b) The conduction mechanism fitting of Al<sub>2</sub>O<sub>3</sub> samples with NH<sub>3</sub> and w/o NH<sub>3</sub> treatment after PDA 900°C in a N<sub>2</sub> ambient

# Chapter 1

## Introduction

### 1.1 General Background

Silicon technology has been the basic of microelectronic and electronics systems for more than thirty years. The density of devices on silicon chip has been following the “Moore’s law”, doubling about every two or three years since about 1980. The density improvement combines not only the progress in lithography but also the innovation in device fabrication technology. Therefore , a steady path of constantly shrinking device dimensions , increasing speed , increasing chip size , and decreasing cost has been found from the Si integrate circuit ( I C ) industry.

Over the years , there have been several major evolutions in silicon digital logic technology. CMOS technology has become the most popular digital logic technology for all IC industry, owing to its low standby power dissipation and scaling properties. Oxide thickness scaling has long been recognized as one of major keys for devices scaling. High drive current and thereby improved device performance can be achieved by reducing oxide thickness. Figure 1.1 shows the expected equivalent oxide thickness ( EOT ) trends from the published 2003-ITRS roadmap.[1] It suggests that at the current rate of progress , we will need EOT of less than 2 nm by 2004 and after 2006 oxy-nitride can’t meet the limit on

gate leakage current density. Such thin gate oxide can not suffer much from extrinsic factors such as defect density, surface roughness and uniformity control. Moreover, the physical limitation of oxide thickness is caused by the quantum mechanical tunneling of carriers. Besides, the direct tunneling current increases exponentially by about one order of magnitude for every 0.2 ~ 0.3nm reduction in oxide thickness. This additional leakage current not only causes increased power dissipation but also may affect the circuit functionality due to the decreased operation margins. For this reason , some of the effective replacement materials for silicon dioxide that are currently being investigated to replace silicon dioxide include  $\text{Al}_2\text{O}_3$  ,  $\text{HfO}_2$ , $\text{ZrO}_2$ , $\text{Ta}_2\text{O}_5$ , $\text{TiO}_2$  .Table 1.1 illustrates basic properties of current high-k material.[2] The alternative high-k material should be thermodynamically stable on Si upon high temperature anneals (needed for dopant activation for polysilicon gates).Unstable dielectric materials will form interfacial layers, which are between the high-k dielectrics and silicon substrate. The high-k film and it's interfacial films would affect various device parameters like effective oxide thickness(EOT),flatband voltage( $V_{fb}$ ),gate leakage current, and channel mobility ,and thus significantly affect the transistor behavior. Some of the metal oxides like  $\text{Ta}_2\text{O}_5$ , $\text{TiO}_2$ ,and BST are known to degrade when annealed at temperature as low as 600°C and have poor electrical properties for MOS devices.[3] The newer high-k materials including  $\text{Al}_2\text{O}_3$ ,  $\text{HfO}_2$ ,  $\text{ZrO}_2$  have generated a lot of interest primarily due to their potential thermal stability in the presence of Si based on thermodynamic considerations.[4][5]

## 1.2 Motivation

The purpose of CMOS scaling is to enhance the performance of circuit and increase the packing density in a chip. However, when scaling down, thinning gate dielectrics inevitably accompany with larger direct tunneling current. The more recent high- $k$  approach is to increase the physical thickness to reduce the direct tunneling current, yet at the same time obtain higher values of gate capacitance by using a dielectric material with a higher dielectric constant (high- $\kappa$ ) relative to  $\text{SiO}_2$ [6]

$$\frac{k_{ox}}{t_{ox}} = \frac{k_{high-k}}{t_{high-k}} \quad \text{[eq-1]}$$

Electrical result on various candidates such as  $\text{Al}_2\text{O}_3$  and  $\text{HfO}_2$  have shown the leakage reduction by order of magnitude, but have encountered the integration challenges such as charge trapping-related threshold voltage instability and mobility degradation.

Many high- $k$  materials have emerged as the most promising gate dielectric candidates for sub 100nm technology due to its superior thermal stability, longer tunneling distance than  $\text{SiO}_2$  at the same EOT and large band gap with a favorable Band alignment. However, the formation of interfacial layer between  $\text{Al}_2\text{O}_3$  and  $\text{SiO}_2$  is still an important issue. Fortunately, as reported, we find adding a nitride layer between oxide/silicon substrate interface can improve reliability.[7][8]



## 1.3 Characterization of Al<sub>2</sub>O<sub>3</sub>

Recently, Al<sub>2</sub>O<sub>3</sub> has gained much attention as promising insulator. The reasons are briefly listed as follows.

### (1) Suitable high dielectric constant :

The reported dielectric constant  $\kappa$  of Al<sub>2</sub>O<sub>3</sub> is about 8 ~10. This magnitude of  $\kappa$ -value is higher than that of SiO<sub>2</sub>( $\kappa$ ~4) and Si<sub>3</sub>N<sub>4</sub> ( $\kappa$ ~7). It is not high enough to induce severe FIBL effect.[9]

### (2) Wide bandgap :

In general, as the dielectric constant increases, the bandgap decreases. The narrower bandgap would increase leakage current. The energy band gap of Al<sub>2</sub>O<sub>3</sub> is about 8.3 eV, which is higher than the other high- $\kappa$  materials such as ZrO<sub>2</sub>, HfO<sub>2</sub> , Ta<sub>2</sub>O<sub>5</sub>. [10][11]

### (3) Acceptable band alignment :

Band alignment determines the barrier height for electron and hole tunneling from gate or Si substrate. For SiO<sub>2</sub>, the band offset of conduction band and valence band is ~9eV, and the barrier height for electrons is 3.5eV and the barrier height for holes is 4.4eV. The high band offset for both electron and hole has the benefit of low leakage current. Figure 1-2 shows the calculated band offsets for most high-k dielectrics.[3] For Al<sub>2</sub>O<sub>3</sub>, barrier height for electron and hole is 2.9eV and 4.3eV, respectively. This band alignment is acceptable and better than other high-k materials such as Ta<sub>2</sub>O<sub>5</sub> and HfO<sub>2</sub>

### (4) High free energy of reaction with Si :

For  $\text{Al}_2\text{O}_3$ , the free energy of reaction with Si is about 64.4 Kal/mole (see Table 1-2).which is higher than that of  $\text{TiO}_2$  and  $\text{Ta}_2\text{O}_5$ [3]. Therefore,  $\text{Al}_2\text{O}_3$  is a more stable material on Si substrate as compared to  $\text{ZrO}_2$ ,and  $\text{HfO}_2$ . [12]-[14]

(5) High heat of formation:

$\text{Al}_2\text{O}_3$  has higher heat of formation (399 kcal/mole). That means that Al is easy to be oxidized to form  $\text{Al}_2\text{O}_3$  and the oxide of Al is usually stable on Si substrate.

According to these profits above discussions, we choose  $\text{Al}_2\text{O}_3$  as the major high-k material and in our investigation. The measurement is performed by MIS capacitor structures.



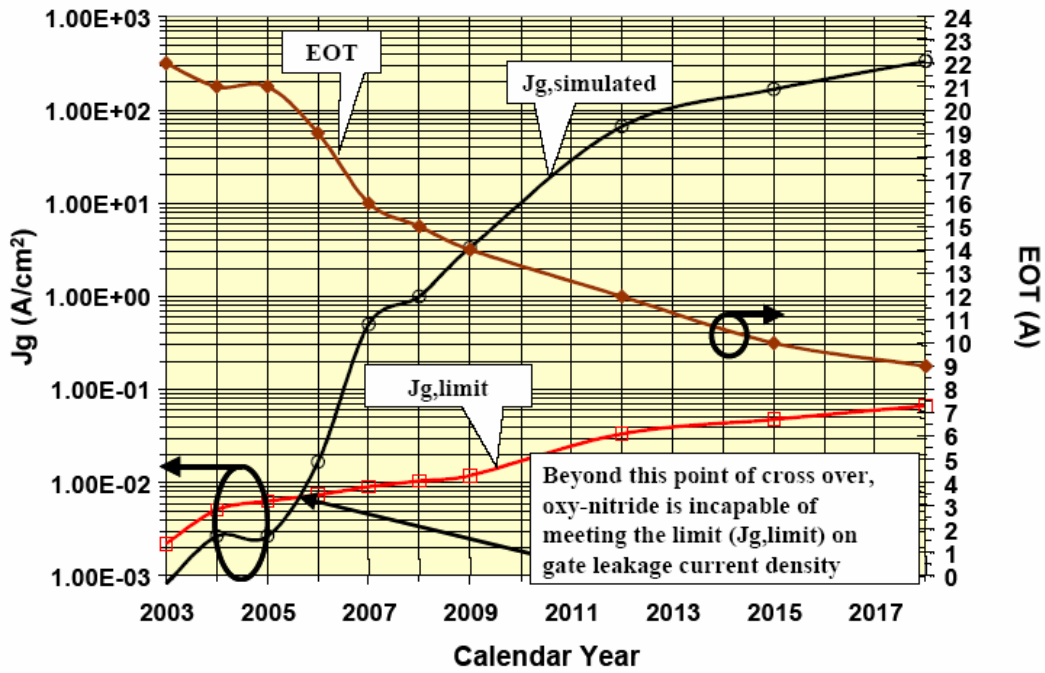


Fig 1.1 the expected equivalent oxide thickness ( EOT ) trends from the published 2003- ITRS roadmap



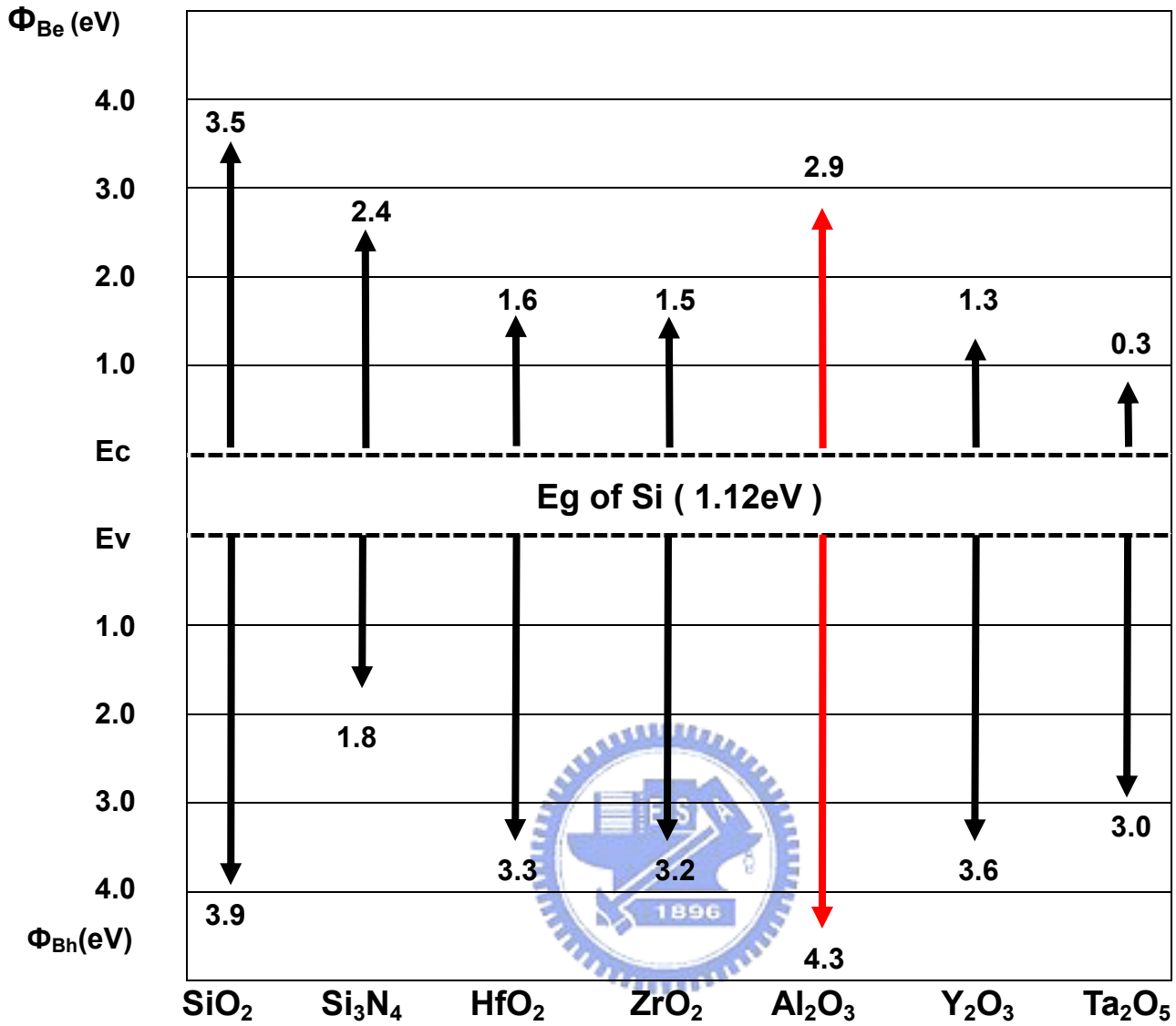


Fig 1-2 Band alignment of topological high-k dielectrics

Material	Dielectric Constsnt(k)	Band gap Eg(eV)	$\Delta E_c$ (eV) to Si	Crystal Structure(s)
SiO <sub>2</sub>	3.9	8.9	3.2	Amorphous
Si <sub>3</sub> N <sub>4</sub>	7	5.1	2	Amorphous
Al <sub>2</sub> O <sub>3</sub>	9	8.7	2.8	Amorphous
Ta <sub>2</sub> O <sub>5</sub>	26	4.5	1-1.5	Orthorhombic
TiO <sub>2</sub>	80	3.5	1.2	Tetrag.
HfO <sub>2</sub>	25	5.7	1.5	Mono.,Tetrag.,Cubic
ZrO <sub>2</sub>	25	7.8	1.4	Mono.,Tetrag.,Cubic

Table 1.1 Basic properties of current high-k candidates[2]

Aspect	Property		
	Al <sub>2</sub> O <sub>3</sub>	ZrO <sub>2</sub>	HfO <sub>2</sub>
Bandgap ( eV )	8.3	5.82	6.02
Barrier Height to Si ( eV )	2.9	1.5	1.6
Dielectric Constant	8-11.5	~25	~30
Dielectric Strength ( MV/cm )	>1.0		2-4.5
Heat of Formation ( Kcal/mol )	399	261.9	271
Δ G for Reduction ( Kcal/mol ) ( MO <sub>x</sub> + Si → M + SiO <sub>x</sub> )	64.39	42.326	47.648
Thermal expansion coefficient ( 10 <sup>-6</sup> K <sup>-1</sup> )	6.7	7.01	5.3
Lattice Constant ( Å ) ( 5.43 Å for Si )	4.7-5.2	5.1	5.11
Self Diffusion Coefficient @ 900°C	1.5048 x10 <sup>-7</sup>	6.0009 x10 <sup>-10</sup>	2.8227x10 <sup>-17</sup>

Table 1-2 Material properties of Al<sub>2</sub>O<sub>3</sub>, ZrO<sub>2</sub>, HfO<sub>2</sub>[3]

## Chapter 2

# Basic Characteristics of Al<sub>2</sub>O<sub>3</sub> Gate Dielectrics Using Rapid Thermal Annealing Technology

### 2.1 Introduction

Recently, MOSFETs with high-k gate dielectrics such as Al<sub>2</sub>O<sub>3</sub>, ZrO<sub>2</sub>, and HfO<sub>2</sub> have been studied intensively. However, investigation of these materials shows that oxygen or dopant penetration through dielectrics is a significant problem due to the low crystallization temperature.[15] In addition, in crystallized gate dielectric films, grain boundaries may act as high oxygen or dopant diffusivity paths, causing device failure with high leakage. For this reason, the high-k materials are expected to have higher crystalline temperature. Among these materials, Al<sub>2</sub>O<sub>3</sub> is a promising candidate because of its compatibility with the poly-silicon gate process and relatively superior scalability. In addition, Al<sub>2</sub>O<sub>3</sub> offers the possibility of pushing the CMOS technology to 10nm feature sizes. As the dielectric constant of Al<sub>2</sub>O<sub>3</sub> is higher than SiO<sub>2</sub>, it will provide a significant increase in capacitance without scaling down the oxide thickness. Rapid thermal Annealing (RTA) is a short time processing technique that can contribute to reduce the thermal budget, low levels of surface roughness, and improve film qualities[16]. It is also very important that RTA is capable of meeting the process integration and manufacturing needs in the currently used CMOS fabrication sequence.

## 2.2 Experiment

The 6-inch P-type Si(100) wafers are after the RCA clean. The high-k material  $\text{Al}_2\text{O}_3$  was then deposited by reactive sputtering in Ar/O ambient. After  $\text{Al}_2\text{O}_3$  deposition, a high temperature post deposition annealing is performed at  $750^\circ\text{C}$ 、 $850^\circ\text{C}$ 、and  $950^\circ\text{C}$  respectively for 30 sec by RTA Rapid Thermal Annealing (RTA). In our experiment, the gate electrode formations were used the Physical Vapor Deposition (PVD) systems. We deposit the TiN film ( $2000\text{\AA}$ ) as the top gate electrode and the thermal evaporation system to deposit the Al film( $5000\text{\AA}$ ) as the backside contact. The cross-sectional view and total experimental procedures of the structure were shown in Fig2-1. At last the Capacitance-Voltage (C-V) and Current-Voltage(I-V) characteristics were measured by HP-4284 and HP-4156C systems. The capacitance equivalent thickness (CET) were extracted from C-V curve.

## 2.3 Results and discussion

### 2.3-1 Capacitance-Voltage characteristic

After the  $\text{Al}_2\text{O}_3$  deposition, the following processes may go through many high temperature treatments during the VLSI fabrication. Such high-temperature treatments are likely to change the morphology and properties of thin films. Fig 2- 2-3 shows the high frequency(100kHz) capacitance-voltage(C-V) ,and Figure 2-4 shows the CET of  $\text{Al}_2\text{O}_3$  samples (without surface treatment) after various post

deposition annealing (PDA) temperature at 750°C, 850°C, 950°C in the O<sub>2</sub> or N<sub>2</sub> ambient. The capacitance of Al<sub>2</sub>O<sub>3</sub> samples annealing in an O<sub>2</sub> ambient decreases with the increasing annealing temperature.[17] Therefore, the CET increases after annealing in an O<sub>2</sub> ambient. This is because an O<sub>2</sub> penetration will induce the increasing of the interfacial layer at Al<sub>2</sub>O<sub>3</sub>/Si-substrate and higher annealing temperature increasing will speed up interface layer growth rate.[18] The exact composition of such interfacial layer is still not known, it is believed its dielectric constant is much lower than Al<sub>2</sub>O<sub>3</sub>. On the contrary, the capacitance of Al<sub>2</sub>O<sub>3</sub> samples annealing in a N<sub>2</sub> ambient is increasing when annealing temperature increases. Therefore, the CET decreases after annealing in a N<sub>2</sub> ambient. The void-defects generated after the sputtered Al<sub>2</sub>O<sub>3</sub> formation and it could be densified followed a RTA process in a N<sub>2</sub> ambient.[19]. A hump is clearly observed in the depletion region of the C-V curve for the 750°C annealing sample. This hump is speculated due to the poor interface quality, and it can be eliminated after a high temperature annealing.

### ***2.3-2 Current density-Electric field characteristic***

The current density (J) in the J-E curve was defined by  $J = I / A$ , where A is the area of capacitor. The CET determined by the C-V measurement. Fig. 2-5 shows the J-E characteristics of Al<sub>2</sub>O<sub>3</sub> film with RTA process in an O<sub>2</sub> ambient. It shows that the thicker Al<sub>2</sub>O<sub>3</sub> film will resist large leakage current, and the lower leakage current was observed.[20] However, the thicker dielectric thickness will reduce capacitance and the driving current. Fig 2-6 shows the J-V characteristics of the fabricated Al<sub>2</sub>O<sub>3</sub> film with RTA in a N<sub>2</sub> ambient. The capacitor can have a lower leakage current with



thinner CET. This is due to RTA process in a  $N_2$  ambient can improve  $Al_2O_3$  film by eliminating void-defect [21][22]. Fig 2-7 shows J versus PDA temperature in the  $O_2$  and  $N_2$  ambient. Obviously, higher PDA temperature can reduce leakage for both annealing ambient. Consequentially, the sputtered  $Al_2O_3$  film can be improved after a  $N_2$  RTA process.

### ***2.3-3 Time Dependent Dielectric Breakdown***

If the leakage current density in the oxide ( $J_{ox}$ ) is kept constant during the stress test (implying that the applied current is held constant), the stress time to breakdown becomes the variable. The length of stress time  $t_{BD}$  elapsed until dielectric breakdown occurred. The time-to-breakdown behavior of a group of oxide samples under such test conditions is referred to as time-dependent dielectric breakdown (TDDB). Gate oxide failure is reported to be a limiting factor for scaling of oxide thickness, since time-to-breakdown decreases with rising gate current. The weibull plot of charge to breakdown for  $Al_2O_3$  samples with various PDA temperature in an  $O_2$  ambient is shown in Fig 2-8. Obviously, distribution of the samples with thinner CET is better than others. However, the level of the charge to breakdown is lower than we expect. Fig 2-9 shows the weibull plot of charge to breakdown for  $Al_2O_3$  samples with various PDA temperature in a  $N_2$  ambient. For various PDA temperature, their distribution and charge to breakdown are almost the same and they are not dependent on  $Al_2O_3$  thickness. This means that the interfacial layer determines the breakdown of the whole stack.[23]

## 2.3-4 Surface morphology

Surface morphology of Al<sub>2</sub>O<sub>3</sub> films which were deposited and followed by different post annealing conditions were shown in AFM analysis. The thickness of the Al<sub>2</sub>O<sub>3</sub> films was about 15nm. According to the published literature[24], smooth surface is desired since roughness will enhance local electric field, which is believed to be detrimental to the gate dielectric integrity. Fig.2-10(a), (b), and (c) show the AFM images of Al<sub>2</sub>O<sub>3</sub> films as deposited with as-deposition , 900 °C PDA in an O<sub>2</sub> ambient, and 900 °C PDA in a N<sub>2</sub> ambient, respectively. The corresponded root-mean-square roughness (R<sub>ms</sub>) values were 0.823 nm, 0.593 nm, and 0.560 nm. The as deposited Al<sub>2</sub>O<sub>3</sub> film show larger roughness. After a PDA process, the roughness of Al<sub>2</sub>O<sub>3</sub> film was improved. Fig.2-11 and Fig 2-12 show the leakage current density at -1V and the R<sub>ms</sub> values of these samples. It was observed that the surface roughness increases when the PDA temperature increases.

## 2.4 Summary

In this chapter, characteristics of the sputtering Al<sub>2</sub>O<sub>3</sub> films with PDA at temperature ranging at 750°C to 950°C for 30 sec are shown, respectively. Higher PDA temperature can effectively reduce leakage current. For the samples with PDA in an O<sub>2</sub> ambient, it will induce extra interface growth to increase CET.[25][26] In a N<sub>2</sub> ambient, the phenomenon won't find. We believe additional RTA in a N<sub>2</sub> ambient technique could suppress the interface growth and improve the gate dielectrics

reliability. The dielectric is shown to be a potential candidate for next generation high-k gate dielectric applications.



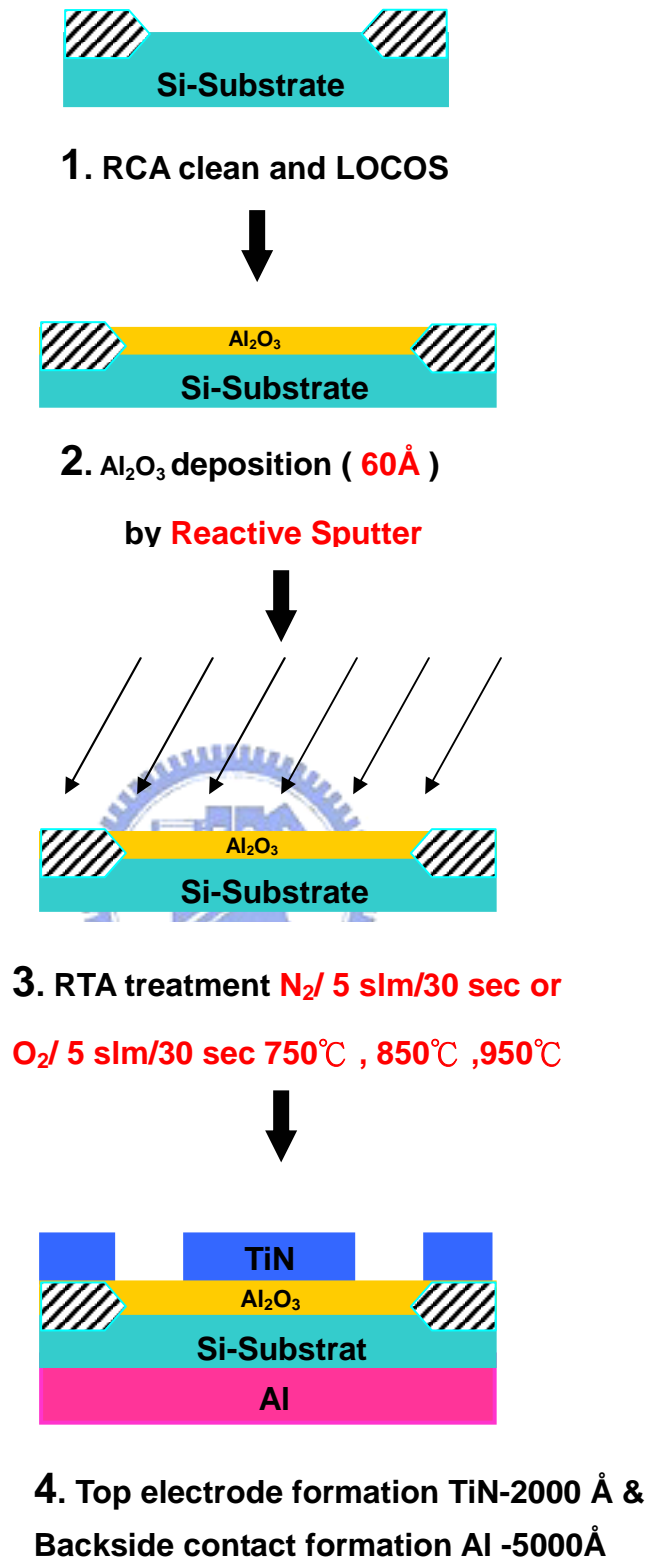


Fig.2-1 Process flows of experimental samples

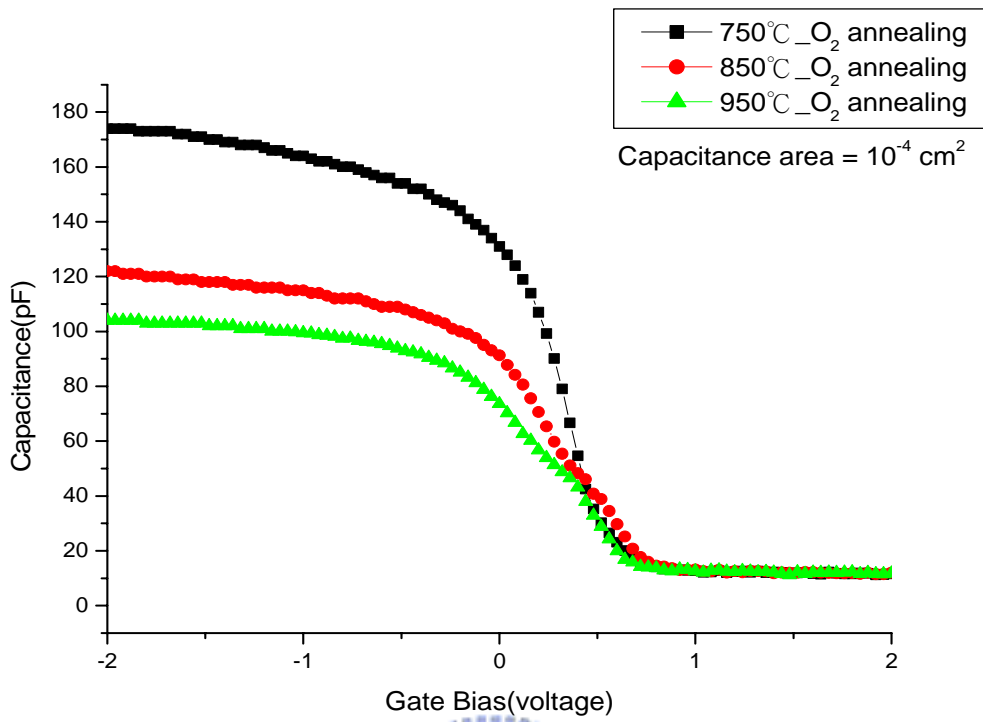


Fig.2-2 The C-V curves of  $\text{Al}_2\text{O}_3$  samples annealing in an  $\text{O}_2$  ambient

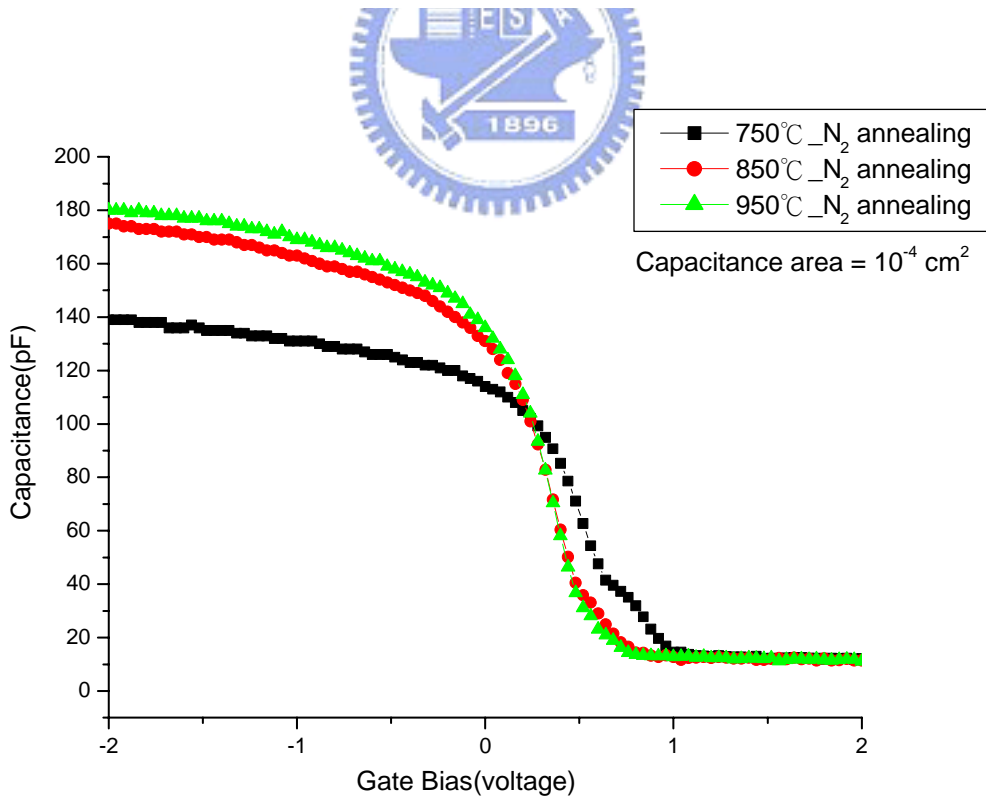


Fig.2-3 The C-V curves of  $\text{Al}_2\text{O}_3$  samples annealing in a  $\text{N}_2$  ambient

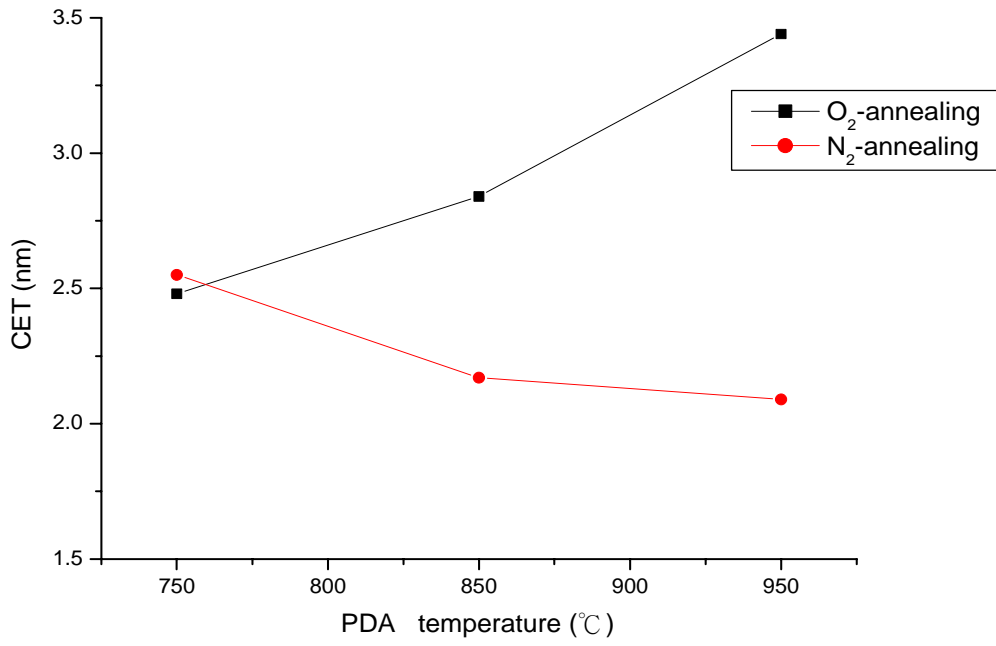


Fig.2-4 The CET of Al<sub>2</sub>O<sub>3</sub> samples after various post annealing temperature 750°C, 850°C, 950°C

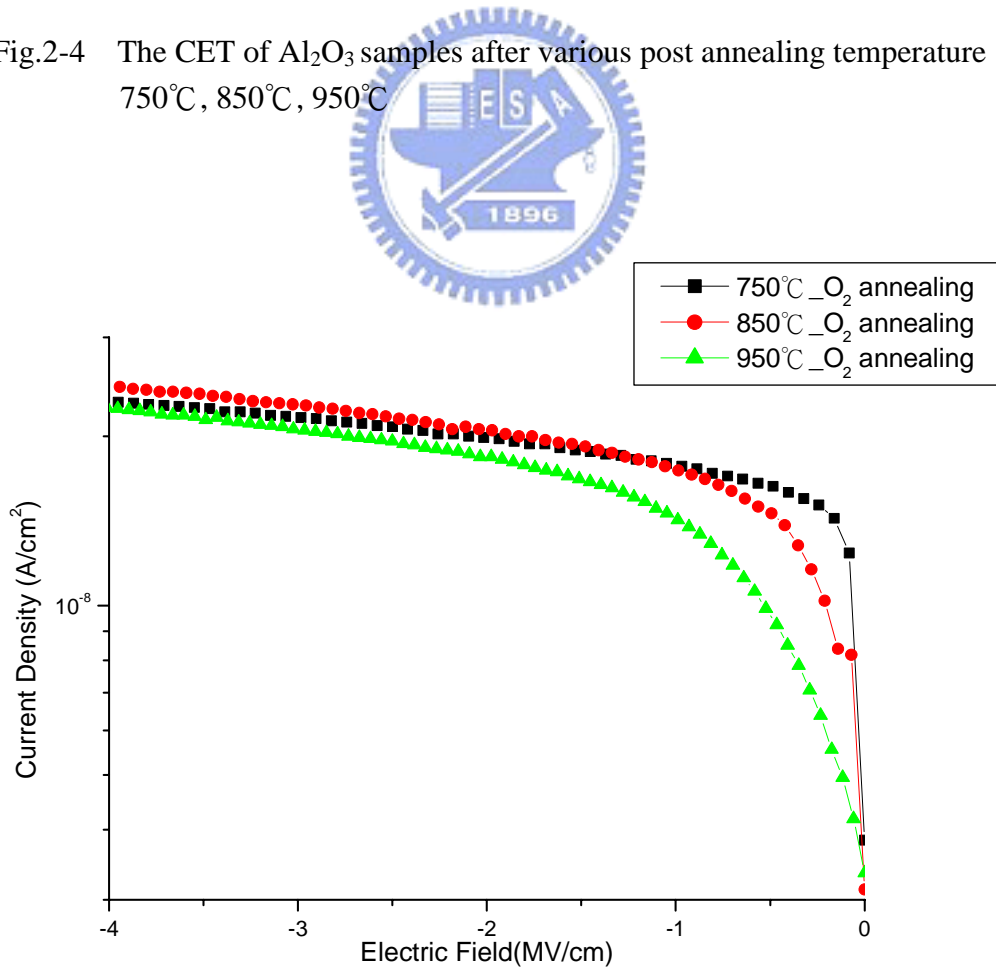


Fig.2-5 The J-E curves of Al<sub>2</sub>O<sub>3</sub> samples with various PDA temperature in an O<sub>2</sub> ambient.

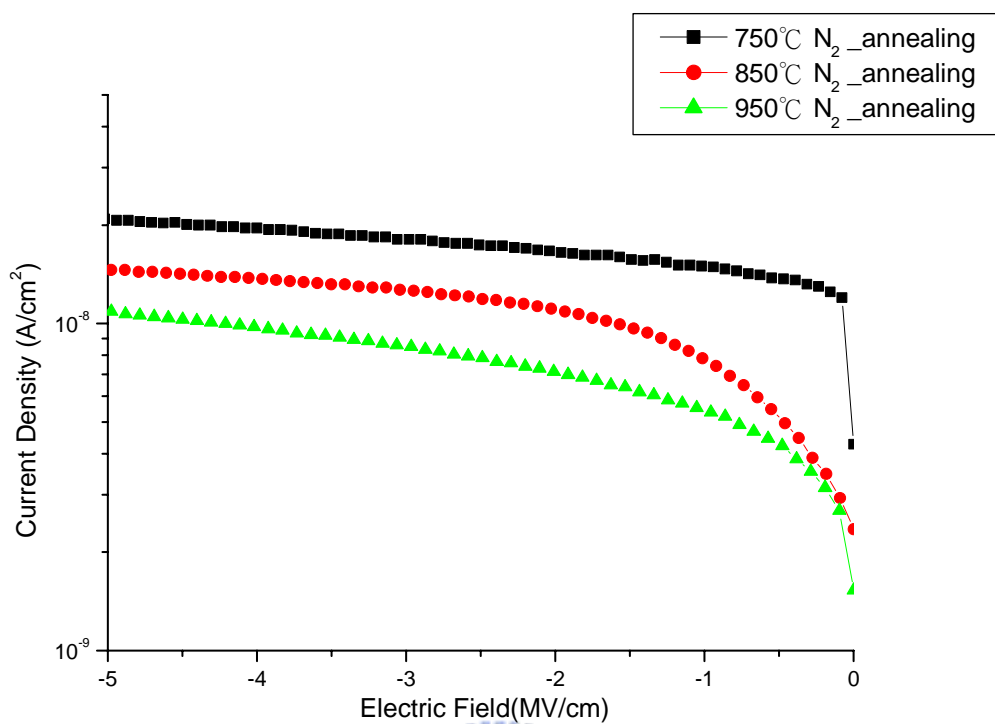


Fig.2-6 The J-E curves of Al<sub>2</sub>O<sub>3</sub> samples with various PDA temperature in a N<sub>2</sub> ambient.

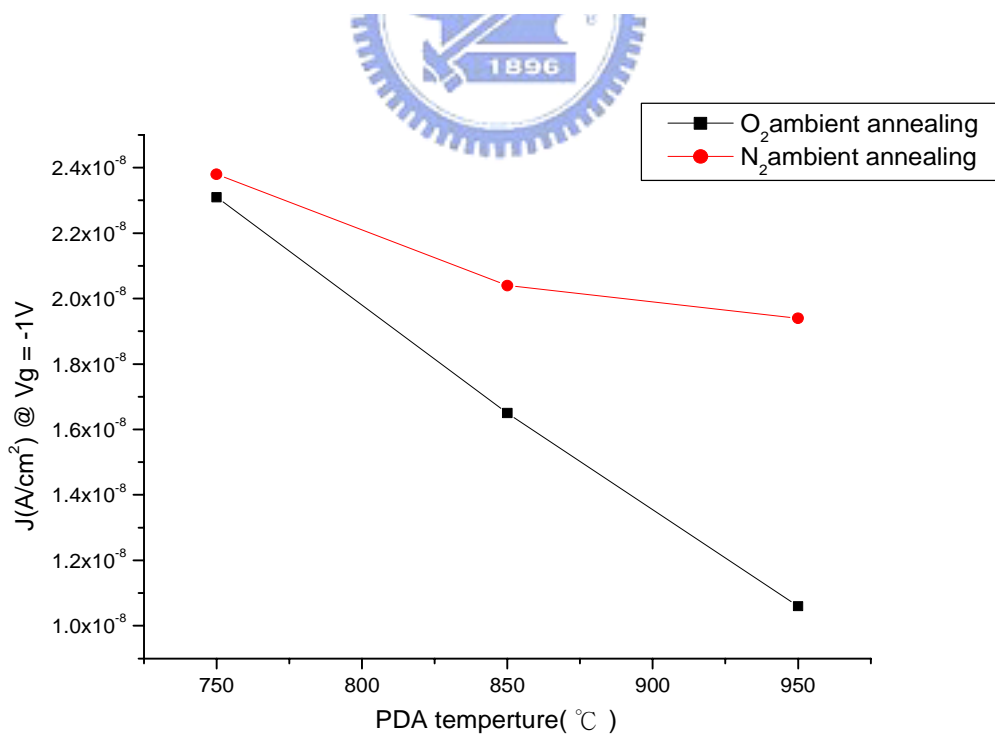


Fig.2-7 The J at V<sub>g</sub> = -1 V of Al<sub>2</sub>O<sub>3</sub> samples with various PDA temperature

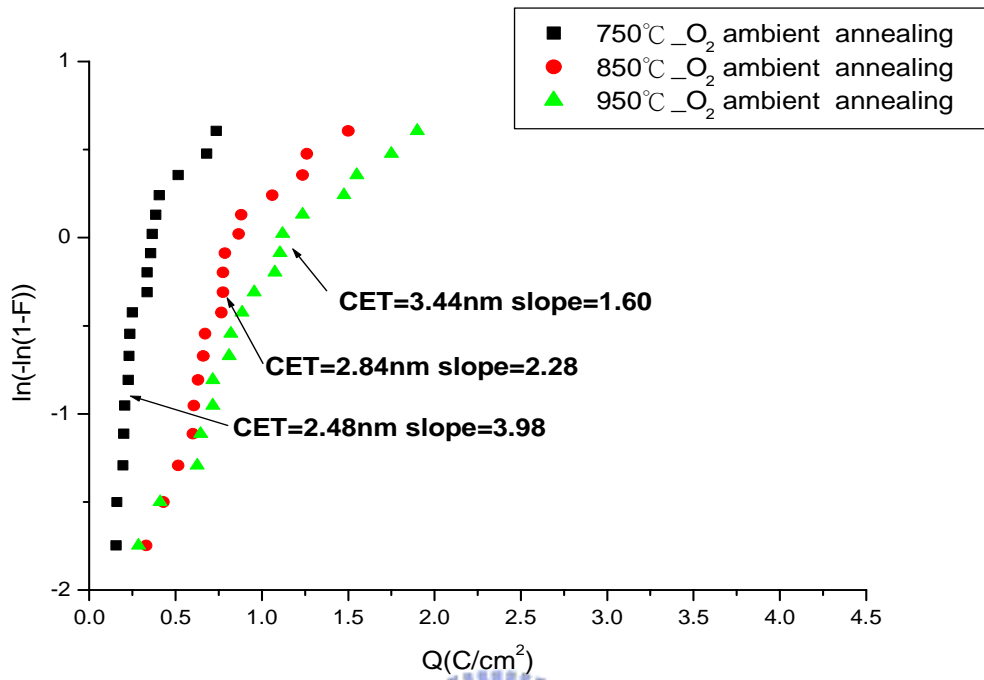


Fig.2- 8 The Weibull plot versus the charge to breakdown  $Q$  ( $C/cm^2$ ) of  $Al_2O_3$  samples with various PDA temperature in an  $O_2$  ambient.

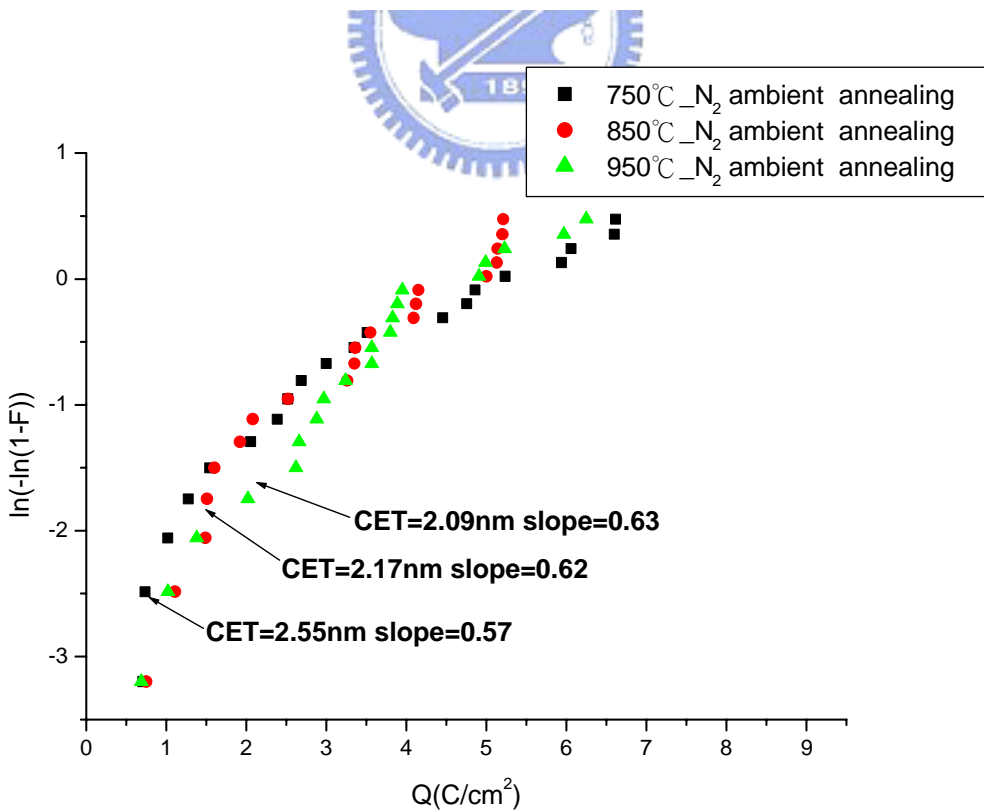
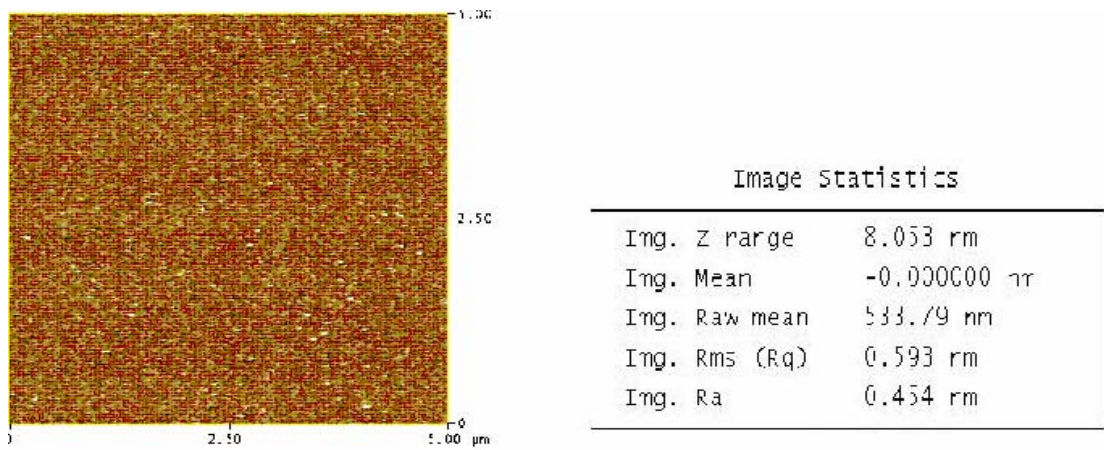


Fig.2- 9 The Weibull plot shows the charge to breakdown  $Q$  ( $C/cm^2$ ) of  $Al_2O_3$  samples with various PDA temperature in a  $N_2$  ambient.

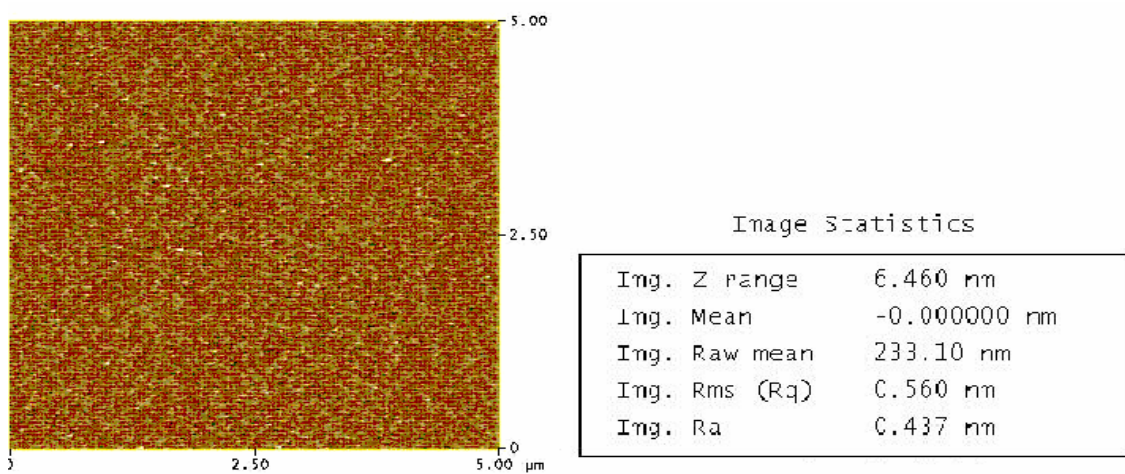




**(a) As deposition**



**(b) O<sub>2</sub>-800°C**



**(c) N<sub>2</sub>-800°C**

Fig.2-10 AFM images of Al<sub>2</sub>O<sub>3</sub> with various PDA: (a) As deposition, (b) O<sub>2</sub>-900°C, and (c)N<sub>2</sub>-900°C

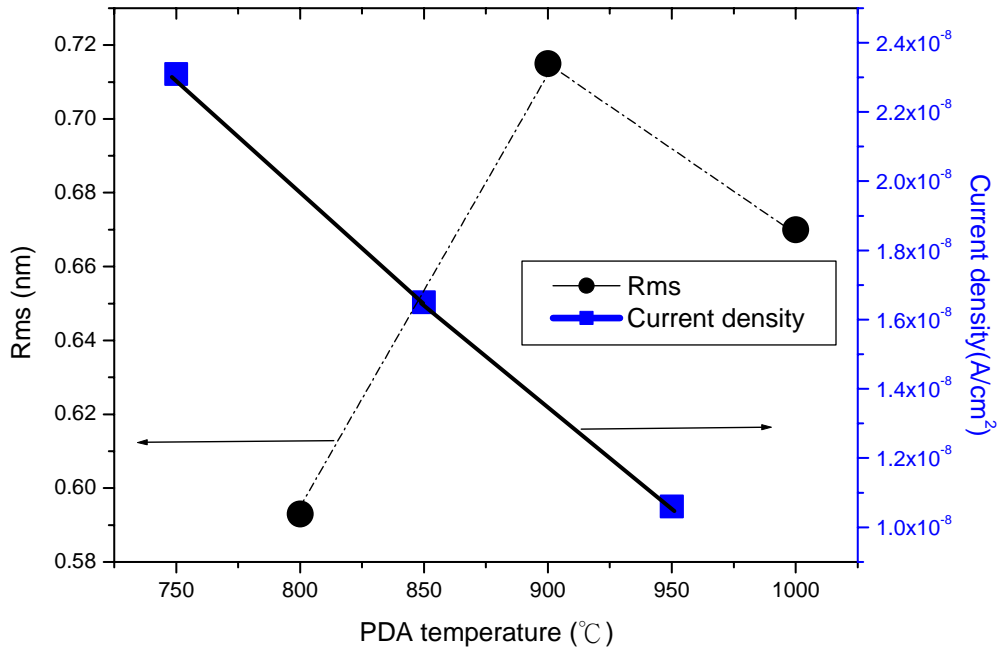


Fig.2-11 Leakage current density,  $R_{ms}$  values versus PDA temperature in an  $O_2$  ambient

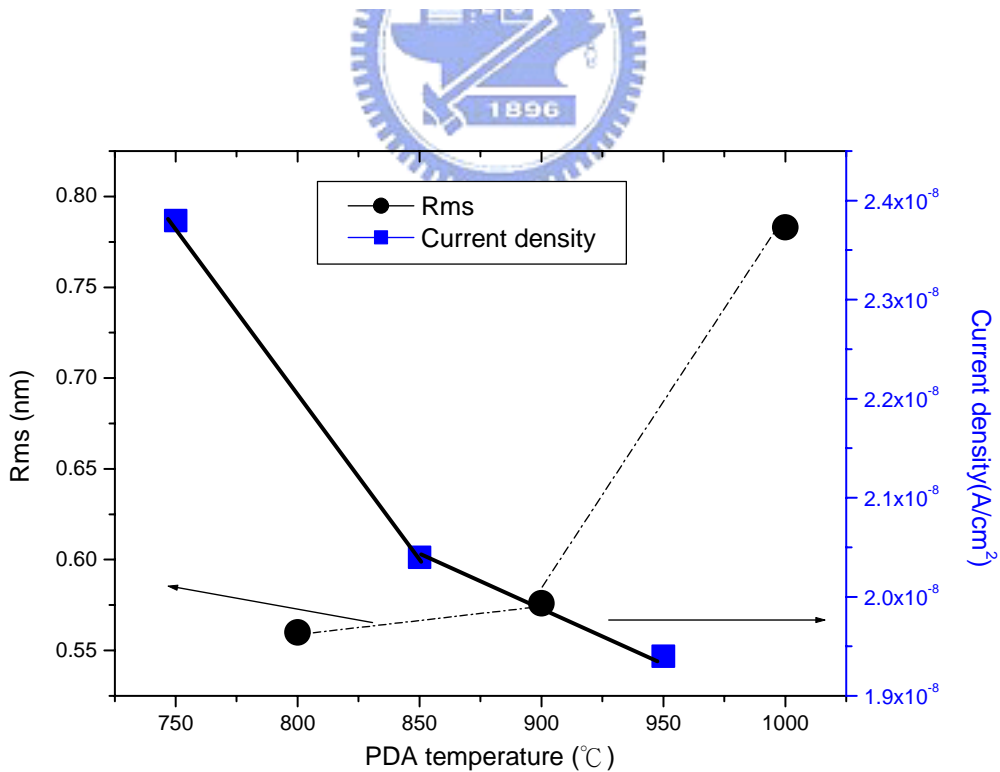


Fig.2-12 Leakage current density, CET and  $R_{ms}$  values versus PDA temperature in a  $N_2$  ambient

## Chapter 3


# Characteristics of Al<sub>2</sub>O<sub>3</sub> Gate Dielectrics Using NH<sub>3</sub> Surface Nitridation Technology

### 3.1 Introduction

As many reports, the direct contact of high-k materials and Si-substrate will be imperfect and have many issues. The dominance of the Si MOSFET over competing technologies has largely been attributed to the high quality of thermally grown SiO<sub>2</sub> and the resulting Si/ SiO<sub>2</sub> interface.[27] The Si/SiO<sub>2</sub> interface is known to have a very low density of interface states ( $D_{it} \sim 2 \times 10^{10}$  states/cm<sup>2</sup>) arising from unsaturated surface bonds and other electrically active imperfections.[27] Interface states lead to degradation of on-current, since carrier mobility is limited by scattering at the interface due to the strong vertical electric fields present in the channel. For maintaining the excellent transport properties at the Si interface, a possible method to suppress the interfacial layer thickness is to passivate the Si surface before Al<sub>2</sub>O<sub>3</sub> deposition. Generally, there are many methods to passivate the Si surface such as surface nitridation, nitrogen-contained ambient annealing, or nitride deposition as the bottom layer. Nitridation of the Si surface using NH<sub>3</sub> treatment before the deposition of high-k materials has been shown to be effective in achieving the low EOT and preventing the boron penetration [28][29] However, this technique results in higher interface charges [30] which leads to higher hysteresis and

reduced channel mobility. In this chapter, we studied the effect of suppressing interfacial layer growth by  $\text{NH}_3$  surface treatments. The  $\text{NH}_3$  treatment would nitridize the Si surface to form a silicon nitride layer. [31]-[33] Silicon nitride is a superior barrier for  $\text{H}_2\text{O}$  and oxygen, and it can suppress oxygen to diffuse into Si substrate.[34] After the  $\text{NH}_3$  treatment, a thin silicon nitride ( $\text{SiN}_x$ ) layer ( $\sim 10\text{\AA}$ ) was deposited and measured by optical measurement system (Ellipsometer). As reports, Nitridation of the Si surface is prior to the deposition of high-k gate dielectrics and it shows the result to achieve the low EOT and increase reliability by making the interface smoother.[35] In this study, the effect of post thermal annealing was studied in the  $\text{O}_2$  and  $\text{N}_2$  ambient, respectively.

## 3.2 Experiment



First, the 6-inch P-type Si(100) wafers were cleaned with standard RCA clean. The samples were divided into two groups. One was without any surface treatment before  $\text{Al}_2\text{O}_3$  deposition, and the other was with a  $\text{NH}_3$  surface treatment before  $\text{Al}_2\text{O}_3$  deposition. The  $\text{NH}_3$ -treatment is performed in high temperature furnace,  $800^\circ\text{C}$  for 1 hour. After  $\text{NH}_3$ -treatment, a  $\text{SiN}_x$  layer ( $\sim 10\text{\AA}$ ) was deposited.  $\text{Al}_2\text{O}_3$  dielectric was then deposited various thickness ( $30\text{\AA}$ ,  $40\text{\AA}$ , and  $50\text{\AA}$ ) by reactive sputtering in the Ar/O (ratio = 24/1) ambient. After  $\text{Al}_2\text{O}_3$  deposition, a high temperature post deposition annealing was performed at  $900^\circ\text{C}$  in the  $\text{O}_2$  or  $\text{N}_2$  ambient. Finally, the gate electrode formation was performed by the Physical Vapor Deposition (PVD) systems. We deposited the TiN film ( $2000\text{\AA}$ ) as the top gate electrode and the thermal evaporation system to deposit the

Al film ( 5000Å ) as the backside contact. The cross-sectional view and total process flow were shown in Fig 3-1. The Capacitance-Voltage (C-V) and Current-Voltage (I-V) characteristics were measured by HP-4284 and HP-4156C systems, respectively. The capacitance equivalent thickness (CET) were extracted from C-V curve. In order to study the conduction mechanism in the Al<sub>2</sub>O<sub>3</sub> film. The current-voltage characteristics with various temperature were measured at room temperature (RT), 50°C , 75°C , 100°C , 125°C , respectively.

### 3.3 Results and discussion

#### 3.3-1 Capacitance-Voltage characteristic

Figure 3-2 shows the comparisons of the C-V curves of the samples with and without surface treatment after PDA 900°C in an O<sub>2</sub> ambient. Both sample shows less hysteresis and hump phenomenon. It is clear that samples with a NH<sub>3</sub> treatment had higher capacitance at strong accumulation than samples without a NH<sub>3</sub> treatment. The CET of Al<sub>2</sub>O<sub>3</sub> film is effectively reduced after NH<sub>3</sub> nitridation since NH<sub>3</sub> surface can suppress the growth of interfacial layer.[36] In Fig 3-2, we can also found the C-V curves shift negatively after NH<sub>3</sub> nitridation can be observed due to the nitridation-induced fixed positive charges[37]. Since positive fixed charges in conventional NH<sub>3</sub> nitridation film is due to N-H bonds at the interface [38]-[40]. Fig 3-3 shows the comparisons of the C-V curves of the samples with or without surface treatment after PDA 900°C in a N<sub>2</sub> ambient. We still can find that the CET of Al<sub>2</sub>O<sub>3</sub> film is effectively reduced after NH<sub>3</sub> treatment.

However, the amount of the C-V curves shift negatively after NH<sub>3</sub> nitridation is decreasing. The reason is due to that PDA in a N<sub>2</sub> ambient will enhance the magnitude of fixed charge in Al<sub>2</sub>O<sub>3</sub> film Fig 3-4 shows the variation of deposited thickness (measured by ellipsometer ) versus CET after PDA 900°C in an O<sub>2</sub> ambient. the NH<sub>3</sub> treatment can effectively reduce the CET despite the initial oxide thickness, which shows the excellent CET scalability of this nitridation process. Because presence of Si<sub>3</sub>N<sub>4</sub> layer can effectively suppress the diffusion of oxygen species into the high-k/Si substrate interface[41]. Without surface nitridation, Al and O atoms are easier to react with Si and are likely to form additional silicon dioxide and/or aluminum silicate layer with relatively lower k value.[42] As the result, the NH<sub>3</sub> nitridation treatment can effectively suppress the interface growth to lower the CET and increases the effective dielectric constant. [43] Fig 3-5 shows the variation of Al<sub>2</sub>O<sub>3</sub> thickness versus capacitance equivalent thickness (CET) after PDA 900°C in a N<sub>2</sub> ambient. We can see almost the same result in an O<sub>2</sub> ambient as in a N<sub>2</sub> ambient, except in a N<sub>2</sub> ambient with higher k value. So the PDA in a N<sub>2</sub> ambient exhibits superior behavior than PDA in an O<sub>2</sub> ambient.

### ***3.3-2 Current density-Electric field characteristic***

Figure 3-6 (a) and (b) show the relationship of gate leakage current versus gate bias after PDA 900°C in the O<sub>2</sub> and N<sub>2</sub> ambient, respectively. The NH<sub>3</sub>-treatment samples show lower leakage current even with thinner CET. It is postulated that the NH<sub>3</sub>-treatment can improve the quality of interface between high-k and silicon substrate and effectively

reduce the leakage current.[44] Fig. 3-7 shows the curve of Current density versus CET curves at  $V_g = -1V$  with  $NH_3$  treatment and without  $NH_3$  treatment. It is clear that  $NH_3$  treatment can effectively reduce leakage current. According to the bonding strength comparisons as follow,  $Si-O(8.42eV) > Si-N(4.75eV) > Si-Si(3.38eV) > Si-H(3.18eV)$ . The Si-N bonds have larger bonding strength than the Si-Si bonds or Si-H bonds. Therefore, we preferred to use the stronger Si-N bonds to replace Si-H bonds, subsequently resist the oxygen diffusion and reduce defect-generation.[45] We also suspect that surface nitridation may effectively reduce the concentration of oxygen vacancies during PDA due to its capability to suppress oxygen diffusion.[42] Therefore, the leakage current will be reduced large. However, as the requirement of the gate dielectric thickness shrinks to below 2nm, the excessive direct tunneling current dominates the gate leakage characteristics and limits scalability of the conventional  $SiO_2$  gate dielectrics. As the result,  $NH_3$  treatment process become potentially to reduce the gate leakage current to meet the request for deep sub-micron CMOS applications.

### ***3.3-3 Time Dependent Dielectric Breakdown***

In this study, the dielectric reliability was also investigated with the behavior of time dependent dielectric breakdown (TDDB). The gate dielectric failure occurred when the significant gate leakage was observed. The magnitude of charge to breakdown ( $Q_{BD}$ ) can be calculated in TDDB measure. Fig 3-8(a) and (b) show the weibull plots of the charge to breakdown ( $Q_{BD}$ ) of  $Al_2O_3$  samples with nearly the same CET after PDA  $900^\circ C$  in

the  $O_2$  and  $N_2$  ambient, respectively. The samples with  $NH_3$  treatment shows more charge to breakdown ( $Q_{BD}$ ). Thus, we suspect that surface nitridation may effectively reduce the concentration of oxygen vacancies during PDA due to its capability to suppress oxygen diffusion.[42] On the other hand, the stronger Si-N bonds bring a stronger interface layer.[35] When part of voltage drop across the  $Si_3N_4$  interfacial layer in samples, the voltage drop across the  $Al_2O_3$  film is lower than expectance, and the influence of the electric field stress is not as severe as the un- $NH_3$  treatment  $Al_2O_3$  samples. As the result, it will enhance the  $Q_{BD}$  for  $NH_3$  treated  $Al_2O_3$  samples. Besides, the slope of the Weibull distribution is an important factor in reliability calculations, where it is used for scaling to total oxide area on chip and low percentiles. A low Weibull slope results in a strong reduction of the  $Q_{BD}$ . A value of slope of 0.9~1.5 is very low for a gate dielectric layer. For thermally grown  $SiO_2$  with a physical thickness of 9 nm, is expected slope = 12 for intrinsic breakdown.[46] Similarly low values below 2 (dotted line) are measured for the other ALCVD high-k layers grown at IMEC as well as for layers reported by other research groups, as citation in Fig.3-9. Breakdown is determined by sputter-induced defects causing weak spots in the  $Al_2O_3$  film. The percolation model is not applicable and the slope values are always low.[47] The sputtered  $Al_2O_3$  film seems to produce a lot of initial defects during a PVD process. Therefore, other deposition technology should be considered such as MOCVD and ALCVD..

### ***3.3-4 Conduction Mechanism***

It is important to study the conduction mechanisms of leakage current in  $Al_2O_3$  film to



improve its electrical and dielectric properties. Comparing the conduction mechanism reported, the current transport mechanism in Al<sub>2</sub>O<sub>3</sub> is still unclear and seems to be strongly process dependent.[48] There may be different conduction mechanisms in the insulator thin film. Typically, two possible effects are in the metal-insulator interface, one is Schottky effect ,the other is Frenkel-Poole effect. The Schottky-Richardson emission generated by the thermionic effect is caused by the electron transport across the potential energy barrier via field-assisted lowering at a metal-insulator interface. The leakage current equation is:

$$J = A^* T^2 \exp\left(\frac{\beta_s E^{1/2} - \phi_s}{k_B T}\right)$$

where  $\beta_s = (e^3 / 4\pi\epsilon_0\epsilon)^{1/2}$ ,  $A^*$  effective Richardson constant,  $\phi_s$  the contact potential barrier. We can find the slope of the leakage current equation.

$$\ln J = \frac{\beta_s}{k_B T} \sqrt{E} + \left[ \ln(A^* T^2) - \frac{\phi_s}{k_B T} \right]$$

$$\text{slope} = \frac{\beta_s}{k_B T}$$

The Frenkel- Poole ( F-P ) emission is due to field-enhanced thermal excitation of trapped electrons in the insulator into the conduction band. The leakage current equation is:

$$J = J_0 \exp\left(\frac{\beta_{FP} E^{1/2} - \phi_{PF}}{k_B T}\right)$$

where  $J_0 = \sigma_0 E$  is the low-field current density,  $\sigma_0$  the low-field conductivity,

$\beta_{FP} = (e^3 / \pi \epsilon_0 \epsilon)^{1/2}$ ,  $e$  the electronic charge,  $\epsilon_0$  the permittivity of free space,  $\epsilon$  the high frequency relative dielectric constant,  $T$  absolute temperature,  $E$  the applied electric field,  $K_B$  the Boltzmann constant,  $\phi_{PF}$  the contact potential barrier. We can find the slope of the leakage current equation.

$$\ln J = \frac{\beta_{FP}}{k_B T} \sqrt{E} + \left[ \ln(J_0) - \frac{\phi_{PF}}{k_B T} \right]$$

$$\text{slope} = \frac{\beta_{FP}}{k_B T}$$

From the equations as shown above, leakage current behaviors of insulate films can be investigated further on the leakage current density ( $J$ )-electric field ( $E$ ) characteristics such as  $\ln J$  vs.  $E^{1/2}$  plots. The plot of the nature log of leakage current density versus the square root of the applied electric field was observed. It is found that the leakage current density is linearly related to square root of the applied electric field. The linear variations of the current correspond either to Schottky emission or to Frenkel-Poole conduction mechanism. For trap states with coulomb potentials, the expression is virtually identical to that of the Schottky emission. The barrier height, however, is the depth of the trap potential well, and the quantity  $\beta_{FP}$  is larger than in the case of Schottky emission by a factor of 2. Distinction between the two processes can be done by comparing the theoretical value of  $\beta$  with the experimental one obtained by calculating the slope of the curve  $\ln J-E^{1/2}$ . The dielectric constant of  $Al_2O_3$  is 7.63 at PDA  $O_2$  ambient and 8.29 at PDA  $N_2$  ambient extracted by Fig 3-4 and-5, the theory  $\beta$  values are  $4.40 \times 10^{-23}$  for Frenkel-Poole and  $2.20 \times 10^{-23}$  for Schottky after PDA in an  $O_2$  ambient and the theory  $\beta$

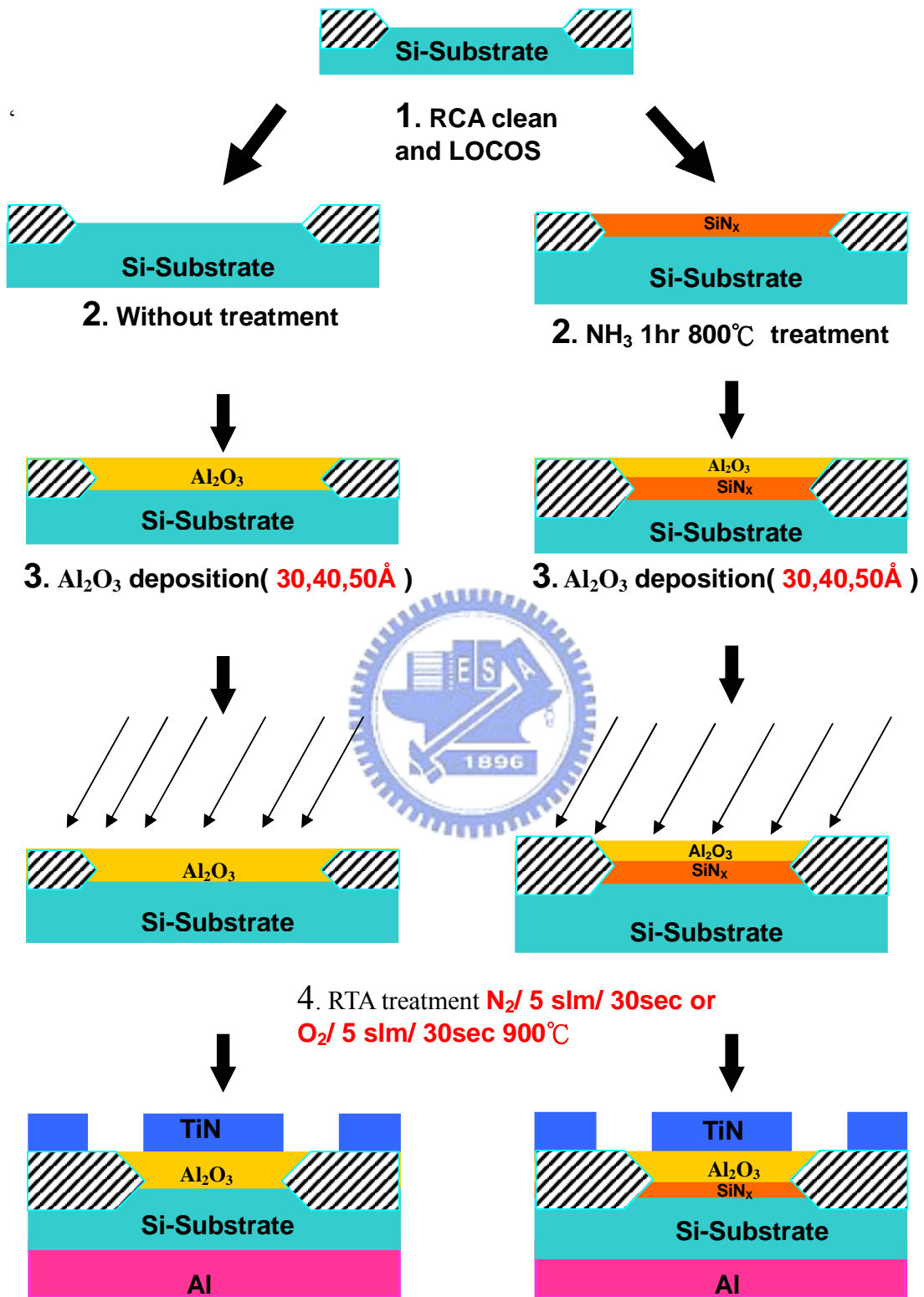
values are  $4.22 \times 10^{-23}$  for Frenkel-Poole and  $2.11 \times 10^{-23}$  for Schottky after PDA in a  $N_2$  ambient. Table 3-1 (a) and (b) shown the experimental  $\beta$  and Schottky barrier high of  $Al_2O_3$  samples with  $NH_3$  and without  $NH_3$  treatment after PDA  $900^\circ C$  in an  $O_2$  ambient and after PDA  $900^\circ C$  in a  $N_2$  ambient ,respectively .Fig 3-10 (a) and (b) show the conduction mechanism fitting of  $Al_2O_3$  samples with  $NH_3$  and w/o  $NH_3$  treatment after PDA  $900^\circ C$  in an  $O_2$  ambient and after PDA  $900^\circ C$  in a  $N_2$  ambient, respectively. We find the conduction mechanism in  $Al_2O_3$  thin film is dominated by Schottky conduction. However, Schottky conduction depends strongly on the barrier between metal and insulator and has the inclination to occur for insulators with fewer defects and a more perfect metal-insulator interface.[49] Samples after  $NH_3$  treatment will have higher barrier high and it is clear that the  $NH_3$  treatment is very effective for improving the interface properties like the barrier height and  $Al_2O_3$  film to reduce the leakage current.[50]

### 3.4 Summery

In this chapter, characteristics of the fabricated  $Al_2O_3$  samples with  $NH_3$  and without  $NH_3$  treatment after PDA  $900^\circ C$  in an  $O_2$  ambient and at PDA  $900^\circ C$  in a  $N_2$  ambient are present, respectively. With surface  $NH_3$  treatment, the CET of  $Al_2O_3$  film can be reduced due to the suppression of interfacial layer growth. In samples with a  $NH_3$  pre-treatment had lower leakage current and better dielectric reliability. Therefore, the  $NH_3$  pre-treatment is a potential technique to improve the performance in high-k gate

dielectric applications.





**5. Top electrode formation TiN -2000 Å pattern contact & Backside contact formation Al -5000 Å contact**

Fig.3-1 Process flows of experimental samples

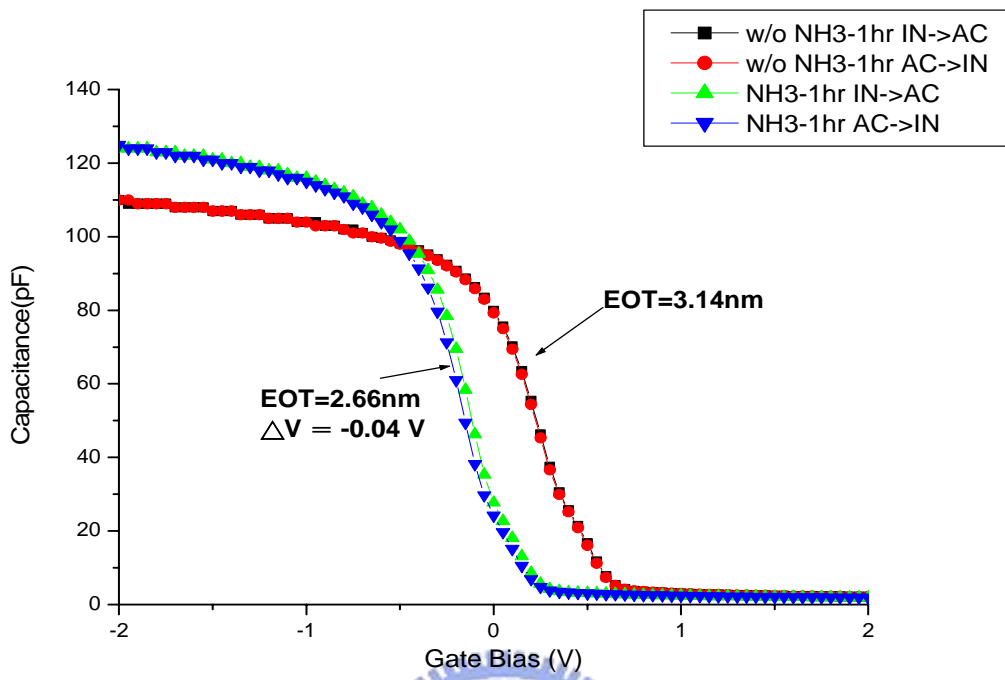


Fig. 3-2: C-V curve of  $\text{Al}_2\text{O}_3$  sample with surface treatment compare to  $\text{Al}_2\text{O}_3$  sample without surface treatment after PDA  $900^\circ\text{C}$  in an  $\text{O}_2$  ambient

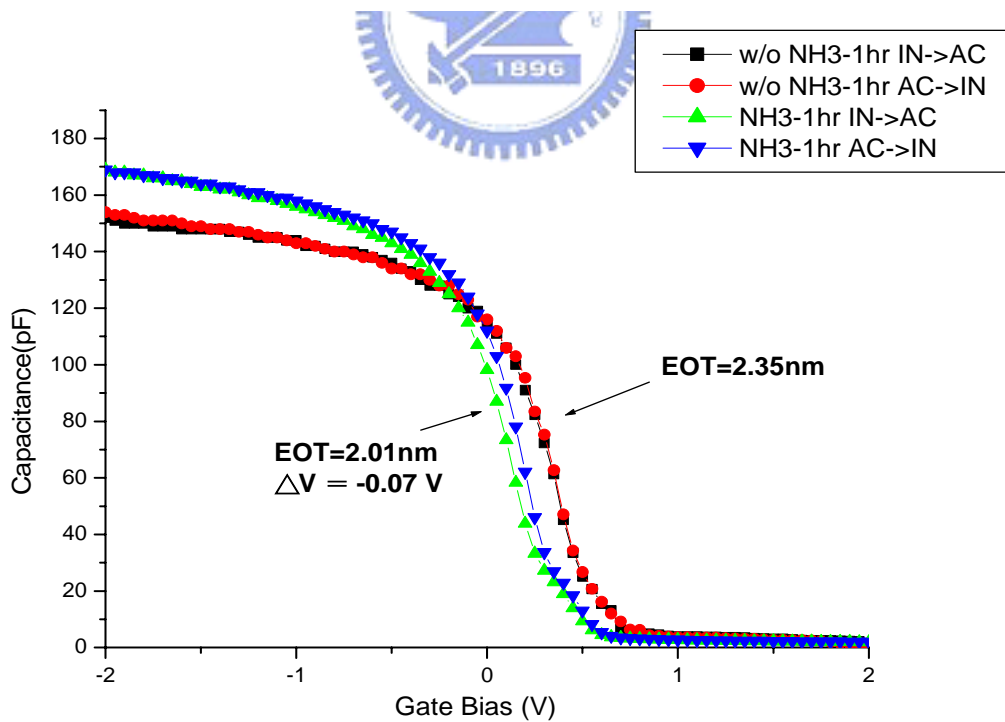


Fig. 3-3: C-V curve of  $\text{Al}_2\text{O}_3$  sample with surface treatment compare to  $\text{Al}_2\text{O}_3$  sample without surface treatment after PDA  $900^\circ\text{C}$  in a  $\text{N}_2$  ambient

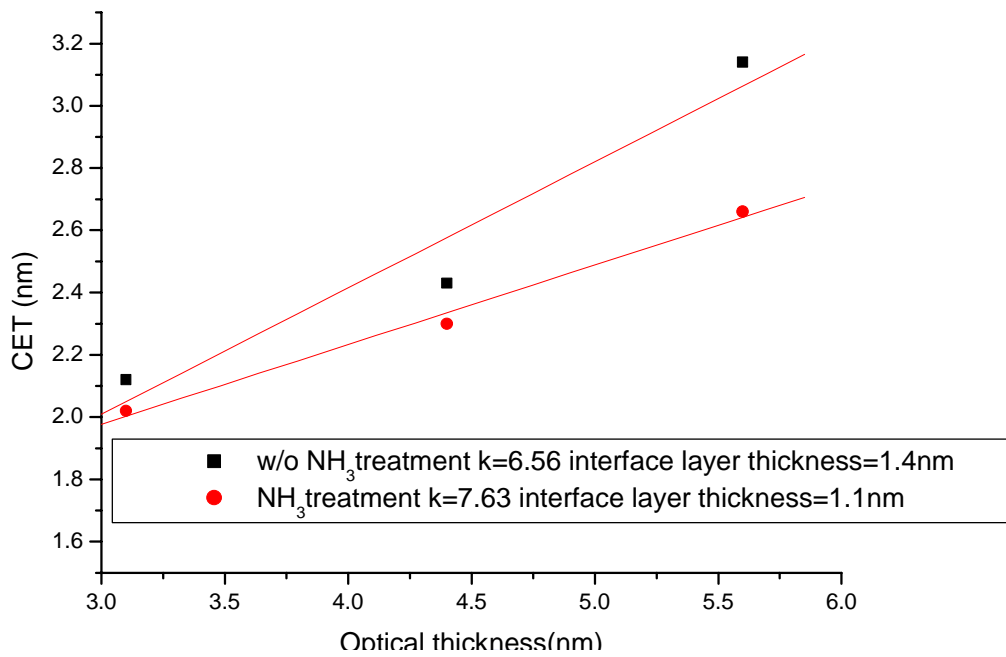


Fig. 3-4: CET versus Optical thickness of Al<sub>2</sub>O<sub>3</sub> sample with surface treatment compare to Al<sub>2</sub>O<sub>3</sub> sample without surface treatment after PDA 900°C in an O<sub>2</sub> ambient

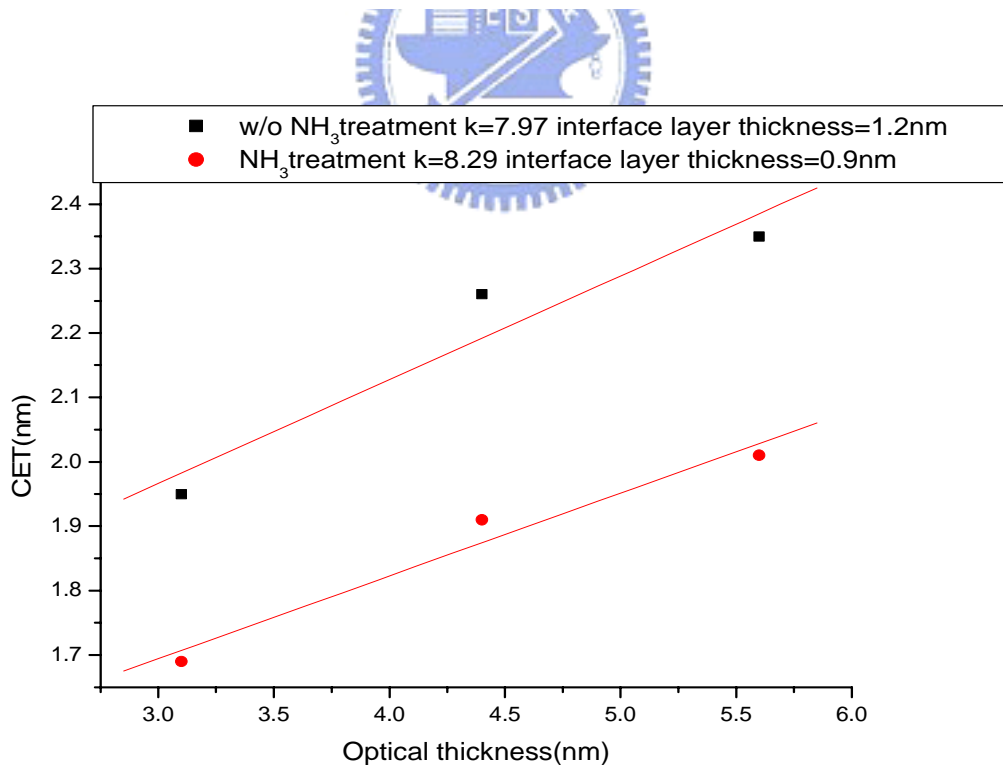


Fig. 3-5: CET versus Optical thickness of Al<sub>2</sub>O<sub>3</sub> sample with surface treatment compare to Al<sub>2</sub>O<sub>3</sub> sample without surface treatment after PDA 900°C in a N<sub>2</sub> ambient

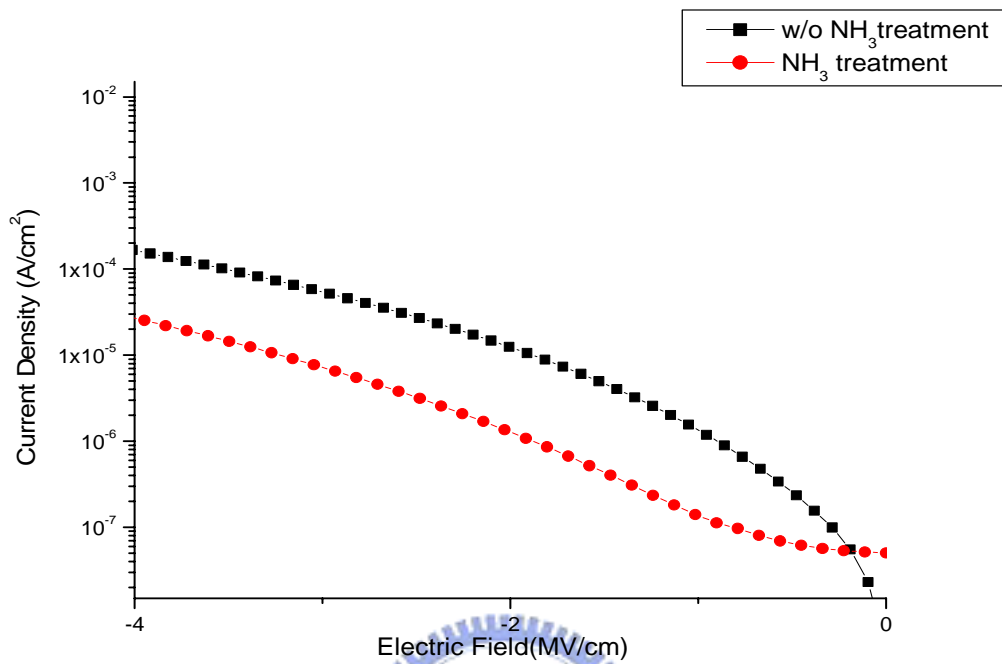


Fig. 3-6-(a): The gate leakage current density (J) versus electric field (E) curves for NH<sub>3</sub> nitrided and w/o NH<sub>3</sub> nitrided after PDA 900°C in an O<sub>2</sub> ambient

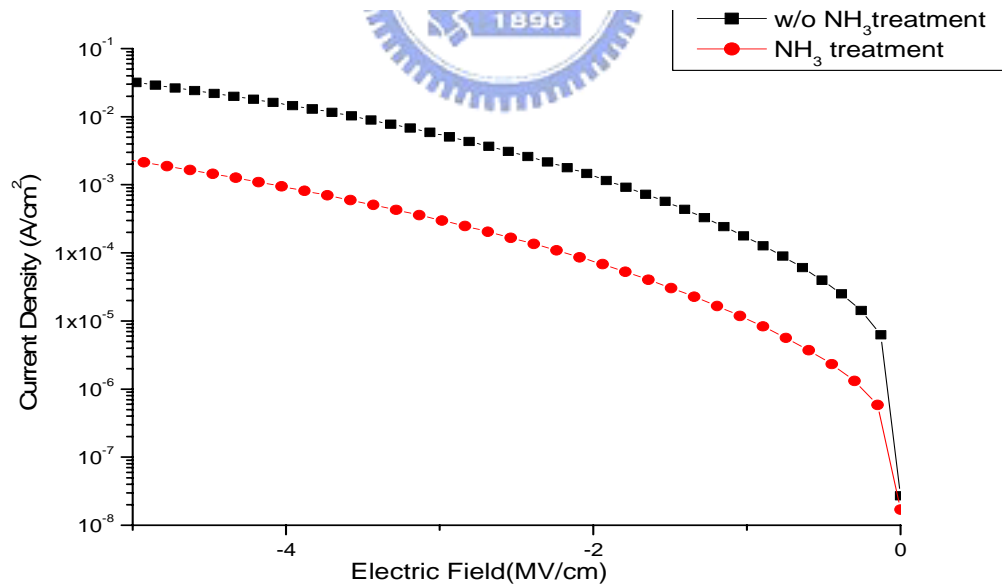


Fig. 3-6-(b): The gate leakage current density (J) versus electric field (E) curves for NH<sub>3</sub> nitrided and w/o NH<sub>3</sub> nitrided after PDA 900°C in a N<sub>2</sub> ambient



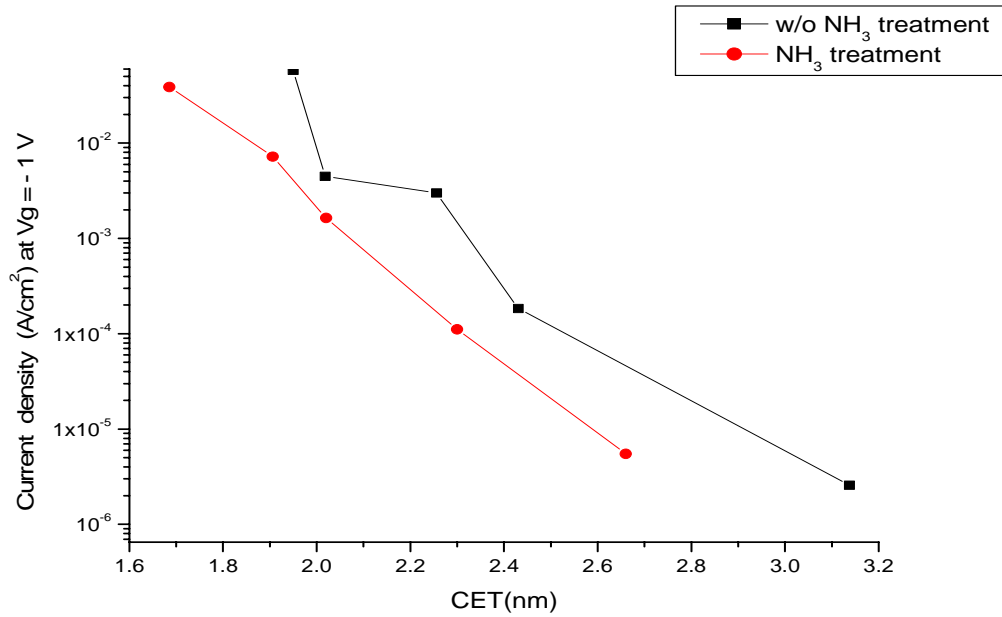


Fig. 3-7 Current density at  $V_g = -1V$  versus CET curves for  $NH_3$  treatment and without  $NH_3$  treatment.

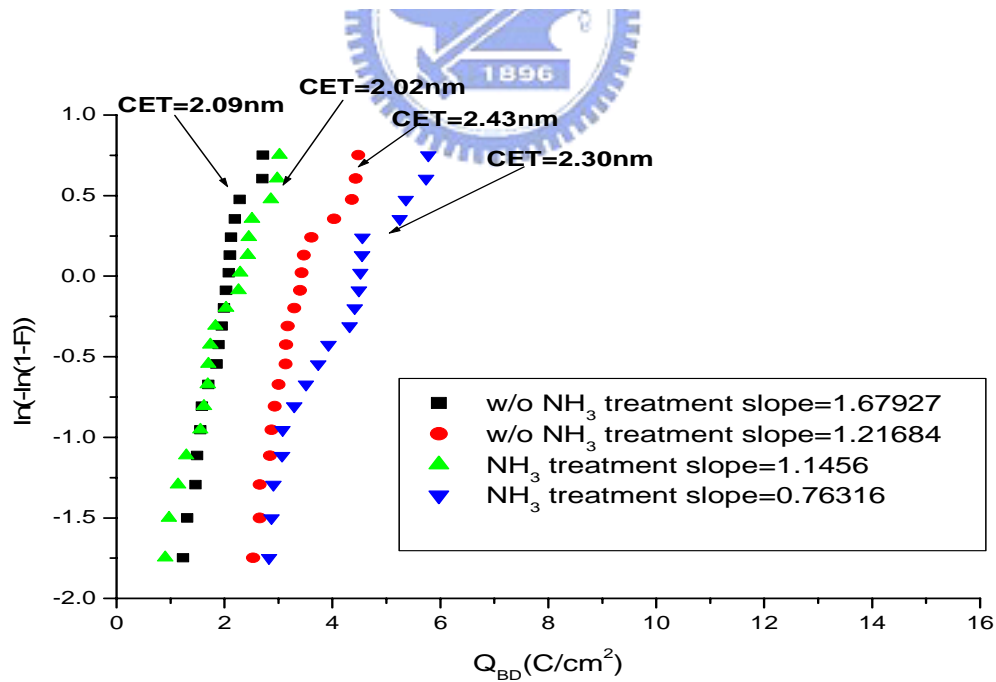


Fig. 3-8 (a) The weibull plot shows charge to breakdown for  $Al_2O_3$  samples with  $NH_3$  and w/o  $NH_3$  treatment at PDA after PDA  $900^\circ C$  in an  $O_2$  ambient

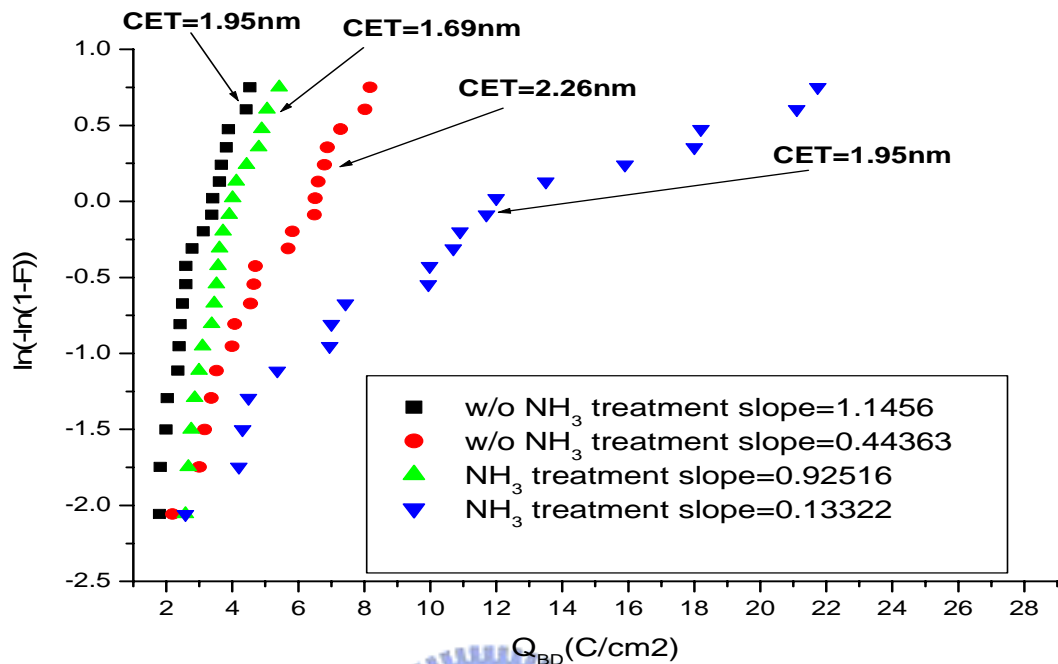


Fig. 3-8 –(b)The weibull plot shows charge to breakdown for  $Al_2O_3$  samples with  $NH_3$  and w/o  $NH_3$  treatment at PDA after PDA  $900^\circ C$  in a  $N_2$  ambient

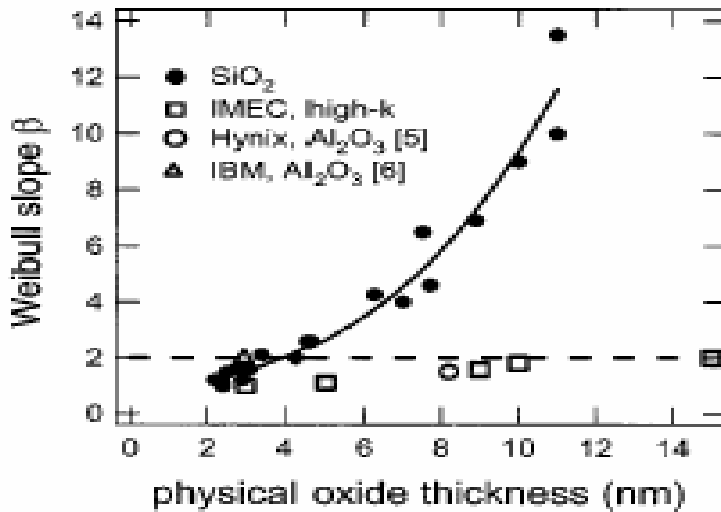


Fig. 3-9. Measured Weibull slopes are plotted versus the physical layer thickness, and a clear gap between the slopes for  $SiO_2$  and the high-k layers can be observed.[20]

	w/o NH <sub>3</sub> treatment		With NH <sub>3</sub> treatment	
	$\beta_{exp}$	Schottky barrier high	$\beta_{exp}$	Schottky barrier high
25°C	$1.88 \times 10^{-23}$	0.71eV	$2.25 \times 10^{-23}$	0.97eV
50°C	$2.18 \times 10^{-23}$	0.72 eV	$2.37 \times 10^{-23}$	1.06eV
75°C	$2.48 \times 10^{-23}$	0.70 eV	$2.49 \times 10^{-23}$	1.13eV
100°C	$2.59 \times 10^{-23}$	0.74 eV	$2.59 \times 10^{-23}$	1.20eV
125°C	$2.71 \times 10^{-23}$	0.70 eV	$2.71 \times 10^{-23}$	1.28eV

Table.3-1(a) The experimental  $\beta$  and Schottky barrier high of Al<sub>2</sub>O<sub>3</sub> samples with NH<sub>3</sub> and w/o NH<sub>3</sub> treatment after PDA 900°C in a O<sub>2</sub> ambient

	w/o NH <sub>3</sub> treatment		With NH <sub>3</sub> treatment	
	$\beta_{exp}$	Schottky barrier high	$\beta_{exp}$	Schottky barrier high
25°C	$1.93 \times 10^{-23}$	0.73 eV	$1.98 \times 10^{-23}$	0.83eV
50°C	$1.83 \times 10^{-23}$	0.65 eV	$2.15 \times 10^{-23}$	0.89eV
75°C	$2.04 \times 10^{-23}$	0.69 eV	$2.32 \times 10^{-23}$	0.96eV
100°C	$2.13 \times 10^{-23}$	0.72 eV	$2.45 \times 10^{-23}$	1.03eV
125°C	$2.01 \times 10^{-23}$	0.77 eV	$2.61 \times 10^{-23}$	1.10eV

Table.3-1(a) The experimental  $\beta$  and Schottky barrier high of Al<sub>2</sub>O<sub>3</sub> samples with NH<sub>3</sub> and w/o NH<sub>3</sub> treatment after PDA 900°C in a N<sub>2</sub> ambient

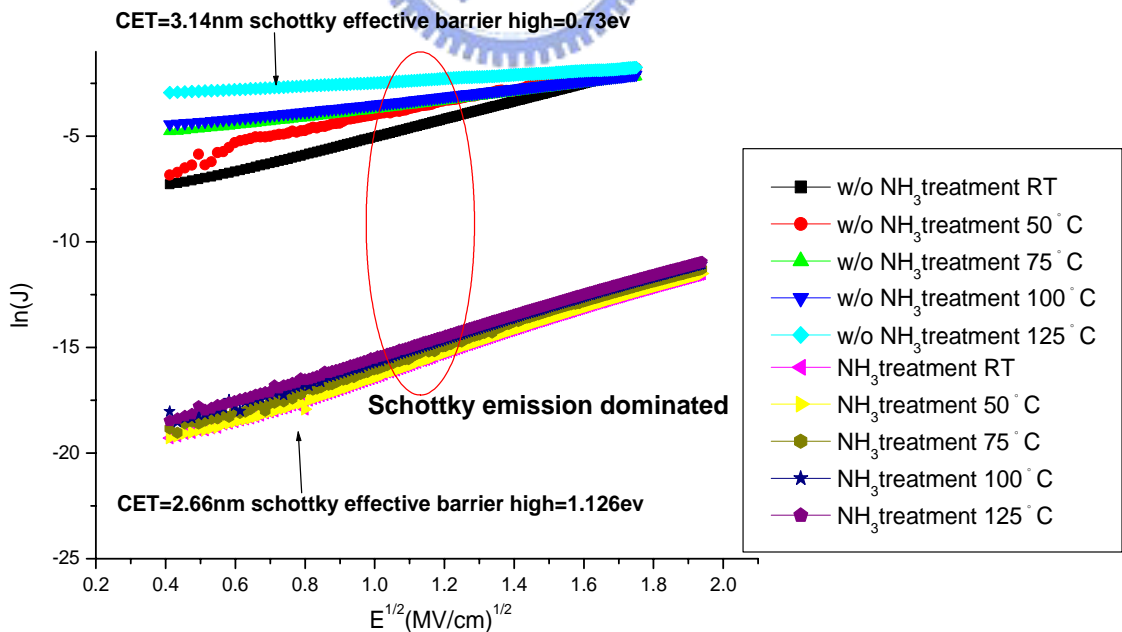


Fig.3-10(a) The conduction mechanism fitting of Al<sub>2</sub>O<sub>3</sub> samples with NH<sub>3</sub> and w/o NH<sub>3</sub> treatment after PDA 900°C in an O<sub>2</sub> ambient

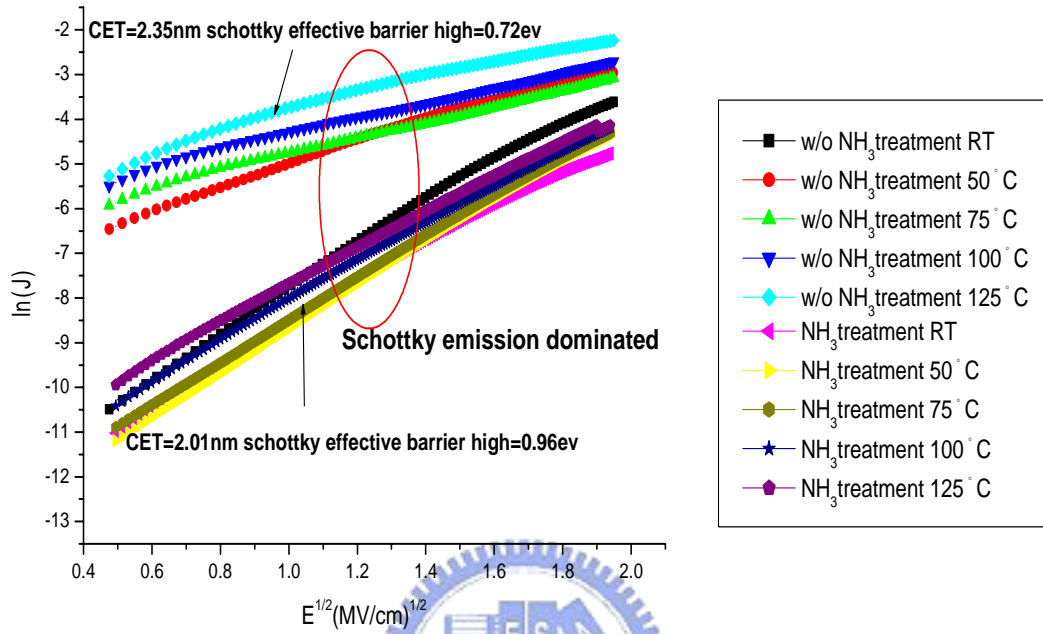


Fig.3-10(b) The conduction mechanism fitting of Al<sub>2</sub>O<sub>3</sub> samples with NH<sub>3</sub> and w/o NH<sub>3</sub> treatment after PDA 900°C in a N<sub>2</sub> ambient

# Chapter 4

## Conclusions and Suggestions for Future Work

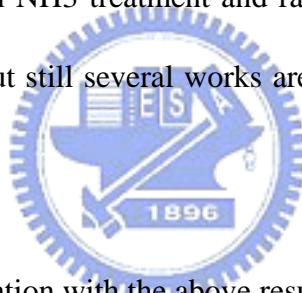
### 4.1 Conclusions

In this thesis, characteristics and reliability of  $\text{Al}_2\text{O}_3$  gate dielectrics with pre-deposition  $\text{NH}_3$  treatment and rapid thermal annealing in  $\text{O}_2$  and  $\text{N}_2$  ambient have been investigated. Several important phenomena were observed and summarized as follows. PDA can effectively reduce leakage current. For the samples with PDA at  $\text{O}_2$  ambient, the interfacial layer increases with the higher PDA temperature. It is obviously that  $\text{O}_2$  penetration will induce the increasing of the interfacial layer at  $\text{Al}_2\text{O}_3/\text{Si}$ -substrate and higher annealing temperature will speed up interface layer growth rate. For samples with PDA in a  $\text{N}_2$  ambient, the void-defect of sputtered  $\text{Al}_2\text{O}_3$  film will be eliminated. The as deposited  $\text{Al}_2\text{O}_3$  film shows larger roughness, and after PDA it will become smoother. However, with higher PDA temperature, surface rough will slightly increase. The surface  $\text{NH}_3$  treatment, can lower the CET value, and reduce the leakage current. In additional, the dielectric reliability was enhanced with  $\text{NH}_3$  treatment. The low Weibull slope of  $\text{Al}_2\text{O}_3$  film may result from sputter-induced defects causing weak spots. Significant process improvements are necessary to enhance dielectric quality ,such as MOCVD, ALCVD. The conduction mechanism in  $\text{Al}_2\text{O}_3$  film was investigated by the various temperature measurement

and fitting. The conduction mechanism in  $\text{Al}_2\text{O}_3$  thin film is dominated by Schottky conduction which occurred for insulators with fewer defects and a more perfect metal-insulator interface. Samples after  $\text{NH}_3$  treatment will have higher barrier height to reduce the leakage current.

## 4.2 Suggestions for Future Work

From recent reports, the major potential show-stoppers for high-k gate dielectrics are considered to be (a) interfacial layer thickness and quality, (b) film morphology after the whole thermal process, (c) reliability issues. Based on the above results,  $\text{Al}_2\text{O}_3$  gate dielectrics with pre-deposition  $\text{NH}_3$  treatment and rapid thermal annealing can have very notable improvement. But still several works are worthy to do in the future and are recommended here.



(1). MOSFET devices fabrication with the above results :

The issues in the integration of  $\text{Al}_2\text{O}_3$ , and its performances can be investigated with the device structures. Mobility is the first concern for considering device performance. Interfacial layer thickness and quality are related to mobility degradation and scaling limit.

(2). More potential interfacial layer investigation :

It is difficult to make a balance between the low leakage current tunneling and the low EOT. The quality of the  $\text{NH}_3$  treatment interfacial layer still could be improved. Moreover, in order to improve the quality at high-k/Si-substrate interface, how to determine the composition of nano-crystals and the boundary layer around crystals is

a key to answer this question.

(3). More potential surface treatment investigation :

For the  $\text{NH}_3$  surface treatment, the excellent improvement of properties are observed. However, the large traps are still existence in  $\text{NH}_3$  surface treatment samples. Other more potential interfacial treatments maybe can be developed to minimize the defects. For example :  $\text{N}_2\text{O}$  gas treatments.

(4). More potential deposition method investigation :

For reactive sputtering in  $\text{Ar}/\text{O}$  ambient to deposit  $\text{Al}_2\text{O}_3$  film, it can not avoid with sputter damages. These damages will become leakage path and can not be accepted to nanometer CMOS fabrication. Other potential manufacturing system like MOCVD maybe can be developed to deposit high quality  $\text{Al}_2\text{O}_3$  film.



## References

- [1] See <http://public.itrs.net/> for most recent updates to the International Technology Roadmap for Semiconductors.
- [2] G.D.Wilk , R.M.Wallace , J.M.Anthony , “ High-k gate dielectrics : current status and materials properties.” Journal of Applied Physics , Vol.89 , No.10, 15 May 2001.
- [3] Jack C.Lee, “Ultra-thin gate dielectrics and High- $\kappa$  dielectrics.”, IEEE EDS vanguard series of independent short courses.
- [4] L. Manchanda ,W.H.Lee ,J.E.Bower “Gate quality doped high K films for CMOS beyond 100 nm: 3-10 nm  $\text{Al}_2\text{O}_3$  with low leakage and low interface states” IEDM 1998
- [5] G. D.Wilk, R. M.Wallace, and J. M. Anthony, “Hafnium and zirconium silicates for advanced gate dielectrics,” J. Appl. Phys., vol. 87, no. 1, pp. 484–492, 2000.
- [6] S. M. Sze, "Physics of Semiconductor Devices\*", 2nd Ed., John Wiley and Sons, (1983)
- [7] Tung Ming Pan “Characterization of Ultrathin Oxynitride (18–21 Å) Gate Dielectrics by  $\text{NH}_3$  Nitridation and  $\text{N}_2\text{O}$  RTA Treatment” IEEE Transactions on electron devices, Vol. 48, NO. 5, May 2001
- [8] S. C. Song, H. F. Luan, C. H. Lee, A. Y. Mao, S. J. Lee, J. Gelpey, S.Marcus, and D. L. Kwong, “Ultra thin high quality stack nitride/oxide gate dielectrics



prepared by in-situ rapid thermal N<sub>2</sub>O oxidation of NH<sub>3</sub> -nitrided Si,” VLSI Technol. Syst. Applica., pp. 78–81, 1999.

- [9] B.Cheng et al, “The impact of high- $\kappa$ / gate dielectrics and metal gate electrodes on sub-100 nm MOSFETs”, IEEE Tran. Electron Device, 46, 1537, (1999).
- [10] Yusuke Morisaki , Yoshihiro Sugita , kiyoshi Irion , Takayuki Aoyoma , “Effects of interface oxide layer on HfO<sub>2</sub> gate dielectrics” , IwGI 2001 Tokyo.
- [11] M. Houssa, V. V. Afanas'ev, and A. Stesmans , “Variation in the fixed charge density of SiO<sub>x</sub>/ZrO<sub>2</sub> gate dielectric stacks during postdeposition oxidation” , Applied Physics Letters -- September 18, 2000 -- Volume 77, Issue 12
- [12] I.Brain and O. Knacke , “Thermochemical properties of inorganic substances.” , Springer , Berlin, 1973.
- [13] L.B.Pankratz, “Thermodynamic Properties of Elements and Oxides (U.S. Dept. of Interior”, Bureau of Mines Bulletin 672, U.S. Govt. Printing Office, Washington, D.C., 1982).
- [14] S. P. Murarka, Silicides for VLSI Applications (Academic, New York, 1983).
- [15] Mohammed Fakhruddin, Rajendra Singh,” Rapid thermal processing of high dielectric constant gate dielectrics for sub 70 nm silicon CMOS technology” IEEE International Conference on Advance Thermal Processing of Semiconductors-RTP 2002.

- [16] D.Damjanovic , K.F.Poole , and R.Singh” Advantages of in-situ rtp for the fabrication of metalhigh-dielectric constant gate dielectric stack for sub 90 nm cmos technology” IEEE Ineternational Conference on Advance Thermal Processing of Semiconductors-RTP 2003.
- [17] G.Lucovsky, Y. Wu, H. Niimi, V. Misra, and J. C. Phillips,” Bonding constraints and defect formation at interfaces between crystalline silicon and advanced single layer and composite gate dielectrics” Appl. Phys. Lett. 74, 2005 (1999).
- [18] Tung Ming Pan “Characterization of Ultrathin Oxynitride (18–21 Å)Gate Dielectrics by NH<sub>3</sub> Nitridation and N<sub>2</sub>O RTA Treatment” Transactions on electron devices VOL. 48, NO. 5, MAY 2001
- [19] Patrick S.Lysaght, Brendan Foran , “Physical characterization of high-k gate dielectric film systems processed by RTA and spike anneal” IEEE Ineternational Conference on Advance Thermal Processing of Semiconductors-RTP 2002.
- [20] S. M. Sze, "Physics of Semiconductor Devices\*", 2nd Ed., John Wiley and Sons, p.442 (1983).
- [21] Y. H. Lin, C. L. Lee, and T. F. Lei, “Monitoring trapped charge generationfor gate oxide under stress,” IEEE Trans. Electron Devices, vol. 44,pp. 1441–1446, 1997.
- [22] Yung Hao Lin; Chung Len Lee; Tan Fu Lei;, “Correlation of stress-induced leakage current with generated positive trapped charges for ultrathin gate oxide,” IEEE Trans. Electron Devices,vol. 45, pp. 567–570, 1998.
- [23] T.Kauerauf, R.Degraeve “Towards understanding degradation and breakdown

of SiO<sub>2</sub>high-k stacks”2002-IEEE

- [24] Shahjahan, M.; Takahashi, N.; Sawada, K.; Ishida, M;” Fabrication and electrical characterization of ultra thin epitaxial  $\gamma$ -Al<sub>2</sub>O<sub>3</sub> gate dielectric films on Si(100) by molecular beam epitaxy (MBE) Extended Abstracts of International Workshop on , 1-2 Nov. 2001
- [25] S. C. Song, H. F. Luan, C. H. Lee, A. Y. Mao, S. J. Lee, J. Gelpey, S.Marcus, and D. L. Kwong, “Ultra thin high quality stack nitride/oxide gate dielectrics prepared by in-situ rapid thermal N<sub>2</sub>O oxidation of NH<sub>3</sub> -nitrided Si,” VLSI Technol. Syst. Applica., pp. 78–81, 1999.
- [26] Liu, C.H.; Hsiu-Shan Lin; Yu-Yin Lin” Extending the reliability scaling limit of gate dielectrics through remote plasma nitridation of N<sub>2</sub>O-grown oxides and NO RTA treatment” Reliability Physics Symposium Proceedings, 2002. 40th Annual , 7-11 April 2002
- [27] G.D.WilK , R.M.Wallace , J.M.Anthony , “ High-k gate dielectrics : current and materials properties.” Journal of Applied Physics , Vol.89 , No.10, 15 May 2001.
- [28] R. Choi, et al., “ High-Quality Ultra-thin HfO<sub>2</sub> Gate Dielectric MOSFETs with TaN Electrode and Nitridation Surface Preparation ”, Symp. VLSI Tech.,p.15,2001.
- [29] K. Onishi et al., “ Dopant Penetration Effects on Polysilicon Gate HfO<sub>2</sub> MOSFET’s ”,VLSI Tech. Dig.P.131, 2001.
- [30] H.-J. Cho, D-G. Park, et al., “ Characteristics of TaOxNy Gate Dielectric with

- Improved Thermal Stability”, Jpn. J. Appl. Phys. Vol. 40, p. 2814, 2001.
- [31] H.-J. Cho, C. S. Kang, K. Onishi, S. Gopalan, R. Nieh, R. Choi, E. Dharmarajan, and J. C. Lee et al, “ Novel Nitrogen Profile Engineering for Improved TaN/HfO<sub>2</sub>/Si MOSFET Performance ”IEDM Tech.,2001, p, 459
- [32] A.L.P. Rotondaro et al., “ Advanced CMOS Transistors with a Novel HfSiON Gate Dielectric ”VLSI Tech.,p.148, 2002
- [33] M. Koyama<sup>1</sup>, K.Suguro, M. Yoshiki, Y.Kamimuta, M. Koike, M.Ohse, C.Hongo and A. Nishiyama<sup>1</sup> et al., “Thermally Stable Ultra-Thin Nitrogen incorporated ZrO<sub>2</sub> Gate Dielectric Prepared by Low Temperature Oxidation of ZrN ”,Tech Digest of IEDM,p.459,2001.
- [34] R. Choi, et al., “ High-Quality Ultra-thin HfO<sub>2</sub> Gate Dielectric MOSFETs with TaN Electrode and Nitridation Surface Preparation ”, Symp. VLSI Tech.,p.15, 2001.
- [35] Tung Ming Pan, “Robust ultrathin oxynitride dielectrics by NH<sub>3</sub> nitridation and N<sub>2</sub>O RTA treatment” IEEE Electron Device Letters, VOL. 21, NO. 8, AUGUST 2000
- [36] Tung Ming Pan “Characterization of Ultrathin Oxynitride (18–21 Å)Gate Dielectrics by NH<sub>3</sub> Nitridation and N<sub>2</sub>O RTA Treatment” Transactions on electron devices VOL. 48, NO. 5, MAY 2001
- [37] C.H. Chen, Y.K. Fang, C.W. Yang, Y. S. Tsair, M.F. Wang, L. G. Yao, S.C. Chen,C.H. Yu, and M.S. Liang, “The 1.3~1.6 nm oxide equivalent gate dielectrics with nitrated oxide prepared by NH<sub>3</sub> nitridation and post-deposition rapid thermal annealing for 0.1μ m and beyond CMOS technology

- application”, Solid State Electronics (SSE), vol. 46, p. 539-544, 2002.
- [38] V. J. Kapoor, R. S. Bailey, and H. J. Stein, “Hydrogen-related memory traps in thin silicon nitride films,” J. Vac. Sci. Technol., vol. A1, pp. 600–603, 1983.
- [39] S. Fujita, T. Ohishi, T. Toyoshima, and A. Sasaki, “Electrical properties of silicon nitride films plasma-deposited from SiF<sub>x</sub>Ny and H source gases,” J. Appl. Phys., vol. 57, pp. 426–431, 1985.
- [40] K. Alloert, A. Van Calster, H. Loos, and A. Lequesne, “A comparison between silicon nitride films made by PCVD of N–SiH<sub>4</sub> /Ar, and N–SiH<sub>4</sub> /He,” J. Electrochem. Soc., vol. 132, pp. 1763–1766, 1985.
- [41] Byoung Hun Lee, Rino Choi, Laegu Kang, Sundar Gopalan, Renee Nieh, Katsunori Onishi, Yongjoo Jeon, Wen-Jie Qi, Changseok Kang and Jack C. Lee et al., “ Characteristics of TaN gate MOSFET with ultrathin hafnium oxide (8Å -12Å) ” IEDM Tech. Dig .,2000
- [42] Yeong Yuh Chen, Chao Hsin Chien, and Jen Chung Lou “High Quality Al<sub>2</sub>O<sub>3</sub> IPD With NH<sub>3</sub> Surface Nitridation” IEEE Electron Device Letters, VOL. 24, NO. 8, AUGUST 2003
- [43] C. T. Liu, E. J. Lloyd, T. Ma, M. Du, R. L. Opila, and S. J. Hillenius, “High performance 0.2um CMOS with 25Å gate oxide grown on nitrogen implanted silicon,” *IEDM*
- [44] S. C. Song, H. F. Luan, C. H. Lee, A. Y. Mao, S. J. Lee, J. Gelpey, S. Marcus, and D. L. Kwong, “Ultra thin high quality stack nitride/oxide gate dielectrics prepared by in-situ rapid thermal N<sub>2</sub>O oxidation of NH<sub>3</sub> -nitrided Si,” VLSI

Technol. Syst. Applica., pp. 78–81, 1999

- [45] S. C. Song, H. F. Luan, Y. Y. Chen, M. Gardner, J. Fulford, M. Allen, and D. L. Kwong, “Ultra thin ( $<20 \text{ \AA}$ ) CVD  $\text{Si}_3\text{N}_4$  gate dielectric for deep-sub-micron CMOS devices”, Tech. Dig. Int. Electron Devices Meet. 1998, p. 373.
- [46] Thomas Kauerauf, Robin Degraeve, Eduard Cartier, Charlotte Soens, and Guido Groeseneken, “Low Weibull Slope of Breakdown Distributions in High-k Layers” IEEE Electron Device Letters, VOL. 23, NO. 4, APRIL 2002
- [47] E. Y. Wu, E. Nowak, L. K. Han, D. Dufresne, and W. W. Abadeer, “Nonlinear characteristics of Weibull breakdown distributions and its impact on reliability for ultra-thin oxides,” in IEDM Tech. Dig., 1999, pp. 441–444.
- [48] J. Kolodzey, E. A. Chowdhury, T. N. Adam, G. Qui, I. Rau, J. O. Olowolafe, J. S. Suehle, and Y. Chen, “Electrical conduction and dielectric breakdown in aluminum oxide insulators on silicon,” IEEE Trans. Electron Devices, vol. 47, pp. 121–128, Jan. 1999.
- [49] Ching-Wu Wang, Shih-Fang Chen, and Ren-De Lin” Effect of Gamma Ray Irradiation on the Conduction Mechanisms of Radio-Frequency-Sputtered  $\text{Ta}_2\text{O}_5$  Films” IEEE Transactions on nuclear science, Vol. 47, No. 4, August 2000
- [50] Yun-Hi Lee, Young-Sik Kim, Dong-Ho Kim , Byeong-Kwon Ju,” Conduction Mechanisms in Barium Tantalates Films and Modification of Interfacial Barrier Height” IEEE Transactions on Electron Devices, Vol. 47, No. 1, January 2000

## 個人簡歷

姓名：謝文斌

性別：男

出生年月日：民國 69 年 7 月 28 日

籍貫：台灣省新竹縣

住址：新竹縣北埔鄉南埔村四鄰 34-1 號

學歷：

國立交通大學材料科學與工程學系學士 (87.9 - 91.6)

國立交通大學電子工程研究所碩士 (91.9 - 93.6)

碩士論文題目：

高介電常數材料氧化鋁在矽基板上之介面特性研究

The Interface Investigation of High-K Material  $\text{Al}_2\text{O}_3$  on Si Substrate